Development of a Surgical Fastener for Rotator Cuff Repair (RCR) Surgery

A Major Qualifying Project Report:
Submitted to the Faculty of the

WORCESTER POLYTECHNIC INSTITUTE

In partial fulfillment of the requirements for the
Degree of Bachelor of Science
By:

Nicholas Brocato

Kristin Gallagher

Gabriela Meza

Emily Viloudaki

Advisor: Dr. Sakthikumar Ambady, WPI
Sponsor: Dr. Robert J. Meislin, NYU

Date: 27April 2017

Rotator Cuff Repair
Tendon-to-Bone Adhesion
Biocompatible

Table of Contents

Authorship

The following report was written in equal contribution by each member of the team. Additionally, each member was prepared for all group meetings, and present during design evaluations and laboratory testing.

Acknowledgements

At this time, the team would like to thank the following WPI Faculty and Staff for assistance and guidance during this project; Elyse Favreau, Lisa Wall, Erica Stults, Dr. José Miguel Lazaro Guevara, Nicholas P. Musselman, and Todd Keiller. Specifically, special thanks to advisor Professor Sakthikumar Ambady, PhD., and sponsor Dr. Robert J. Meislin (Langone Medical Center, NYU).

Abstract

With an increasing need for rotator cuff surgeries to be performed on a variety of patient demographics, an adaption to current surgery technique is necessary, as sutures commonly pull through the healing tendon, often leading to a secondary repair surgery. If this second surgery is conducted, the range of motion in the shoulder joint becomes limited, the rehabilitation process is extended, and time and money are wasted. This Major Qualifying Project aims to develop a biocompatible surgical fastener to reattach the affected tendon into its insertion point with compatible mechanical properties that will work cohesively with the current surgical procedures.

Table of Figures

Table of Tables

1 INTRODUCTION

Rotator cuff repair (RCR) surgeries are traditionally performed using suture anchors and non-biodegradable sutures to hold an elongated piece of damaged supraspinatus tendon down to the shoulder bone. With this surgical method of rotator cuff repair, the major cause of a Type I retear is from the sutures pulling through the tendon due to a high stress concentration at the suture-tendon interface. Unfortunately, tendon retears occur in at least 6% of patients, and the percentage is even higher in patients who undergo RCR for large to massive tears (Mahure *et al*., 2016). This project aims to develop a technology that reduces Type I retear rates in patients with large to massive, 3 centimeters in length or greater, tears.

The team worked with advisor, Dr. Sakthikumar Ambady, and sponsor, Dr. Robert J. Meislin, an orthopedic surgeon at New York University Langone Medical Center, who has extensive experience with rotator cuff repair surgeries. The project inception was derived from Dr. Meislin's published patent on a "velcro-like" hook-and-loop fastener concept for application to RCR repair. Conceptually, the "velcro-like" design will allow for tendon-to-bone adhesion over a larger area, thereby reducing stress concentrations and subsequent retears. The team considered this concept, among others, during the design and testing processes.

Ultimately, the goal of this product is to obtain reproducible data indicating that the final design is biocompatible and minimizes the instances of Type I retears in RCR patients with large to massive tears. Data on developed prototypes will be obtained through *in vitro* biocompatibility tests, Instron tensile testing, and computerized modeling using finite element analysis.

2 LITERATURE REVIEW

2.1 Anatomy

The rotator cuff consists of four muscle-tendon units: the supraspinatus, infraspinatus, subscapularis, and teres minor. Each tendon is named after its respective muscle; for instance, the supraspinatus tendon is the tendon responsible for connecting the supraspinatus muscle to the humeral head (Vollans *et al.*, 2016). The muscles can be visualized in Figure 1 below.

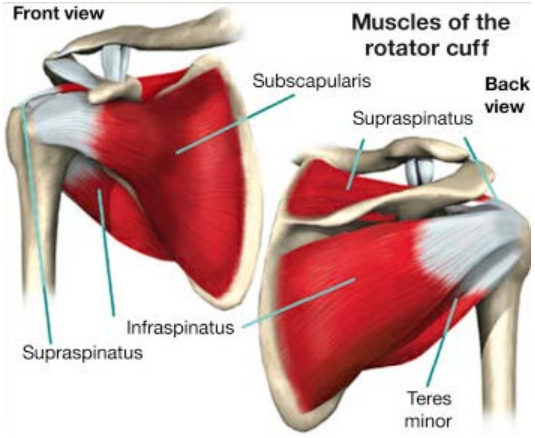

Figure 1. Muscles of the Rotator Cuff. (Vollans *et al.*, 2016)

All of the muscles arise from the scapula and their tendons insert into the humeral head. As seen in Figure 1, the supraspinatus and infraspinatus originate from posterior region of the scapula, and insert onto the greater tuberosity. Crucially, the subscapularis is located directly inferior to the acromion process, a significance that can often result in a rotator cuff injury. The proximity to the acromion results in great amounts of friction against the supraspinatus, and ultimately can result in a full or partial tear. The teres minor originates from the lateral border of the scapula and inserts onto the interior facet of the greater tuberosity. Lastly, the subscapularis originates on the anterior region of the scapula and inserts on the lesser tuberosity and humeral neck medial to the long head of the biceps tendon (Vollans *et al.*, 2016). Functionally, the supraspinatus is responsible for abduction of the glenohumeral joint, the infraspinatus and teres minor are responsible for external rotation of the glenohumeral joint, and the subscapularis is responsible for internal rotation of the glenohumeral joint (Vollans *et al.*, 2016).

2.2 Pathophysiology of Initial Tears

Initial tears of the rotator cuff originate due to several intrinsic and extrinsic factors pertinent to the affected patient. Intrinsic factors are difficult to account for with surgery, as they fundamentally involve a decrease of the tendon's integrity. Extrinsic factors can be associated with a perfectly healthy tendon, and result in a tear due to factors such as impingement or mechanical overuse. These factors along with the classification of tears are outlined in the proceeding sections.

2.2.1 Extrinsic Factors

There exist various intrinsic and extrinsic factors that lead to the onset of rotator cuff damage. Extrinsically, impingement and mechanical overuse are critically responsible for rotator cuff trauma and in severe cases results in cases that require surgical intervention. Impingement is primarily observed as a factor associated with the supraspinatus and specifically is due to its anatomical location (Yadav *et al*., 2009). The supraspinatus passes inferior to the acromion process, and due to certain morphologies of the acromion process, the supraspinatus tendon becomes pinched against the acromion. The morphologies of the acromion process include Type I (flat), Type II (curved), and Type III (hooked). In a study performed by Bigliani regarding the relationship of acromial architecture and rotator cuff disease, 17%, 43%, and 39% of rotator cuff tears resulted from Type I, Type II, and Type III acromion processes, respectively (Bigliani, *et al.*, 1991). There exists a correlation between the morphology of the acromion process and the instance rate of a full or partial tear of the supraspinatus tendon. As a preventative procedure, subacromial decompression is performed quite often in rotator cuff surgery, not only to decrease the factors associated with impingement, but to also help visualize the supraspinatus tendon before reinserting it into the humeral head (Yadav *et al.*, 2009). Impingement affects the supraspinatus tendon almost exclusively, and directly results from the morphology of the acromion process, and the fundamental location of the supraspinatus, that is, how it passes inferior to the acromion, and when under tension due to abduction of the glenohumeral joint, forces strongly against the acromion.

Mechanical overuse is another critical factor associated with rotator cuff disease. Most (64%) of individuals presenting symptoms of a full thickness rotator cuff tear had a full thickness tear affecting their dominant arm. Despite this, a significant number of patients (36%) displaying

symptoms of a full thickness cuff tear were affected on their non-dominant side, and 28% of those individuals were affected on their non-dominant side only (Harryman *et al*., 1991). 70% of full thickness tears occurred in sedentary individuals (Yadav *et al*., 2009). While it is expected that active individuals would have more opportunity to tear their rotator cuff, it is unsurprising that sedentary individuals would have a higher instance rate of being affected. Especially when considering the following intrinsic factor associated with the pathophysiology of rotator cuff disease, primarily when taking the degenerative microtrauma theory into consideration.

As an aside, patients who are sedentary with minimal weakness will seldom require surgical intervention to repair a torn rotator cuff. Logically, those who are more active are in greater need of a functional, non-impaired rotator cuff and will require surgical intervention (Vollans *et al.*, 2016). Moreover, sedentary patients likely do not need full mechanical integrity of their rotator cuff due to a decreased level of mechanical loading; therefore, surgeons will usually opt for a less invasive, less risky physical rehabilitation approach.

2.2.2 Intrinsic Factors

Coupled with mechanical overuse is the degenerative microtrauma theory. This theory is fundamentally based around the idea that when fibers of a tendon tear, the remaining fibers assume the load that the now severed fibers had. The increased load causes more fibers to tear in an iterative process, leading ultimately to a full rotator cuff tear (Yadav *et al*., 2009). Mechanical overuse leads to the initial fiber tears, prompting the onset of degenerative microtrauma.

There also exists a strong correlation between age and the applicability of the degenerative microtrauma theory and ultimately the prevalence of cuff tears. Epidemically, only 4% of patients under 40 years of age showed signs of a complete rotator cuff tear, while the instance rate rose to 54% in patients aged greater than 60 years (Vollans *et al.*, 2016). In a study completed by Tempelhof, the frequency of rotator cuff tears “increased from 13% in the youngest group (age 50-59) to 20% (age 60-69), 31% (age 70-79) and 51% in the oldest group (80-89)” (Tempelhof *et al.*, 1999). There is a distinct positive correlation between the age of the individual and the onset of rotator cuff disease. There are multiple intrinsic factors that led to this observation, and have been observed in cadaveric studies. Age-related factors observed in these cadavers are not limited to: thinning and disorientation of the collagen fibers, myxoid

degeneration, hyaline degeneration, vascular proliferation, fatty infiltration, chondroid metaplasia, and calcification (Yadav *et al*., 2009).

Degeneration is a critical factor associated with the onset of rotator cuff disease. Likewise, impingement is equally, and mostly regarded as a cofactor to the onset of rotator cuff disease. That is, both theories apply to the onset of the disease concurrently (Vollans *et al.*, 2016). According to Vollans, Codman describes a critical factor in degeneration as hypovascularisation of the distal supraspinatus enthesis. Moreover, the critical zone of hypovascularisation occurs one centimeter or greater from the insertion of the supraspinatus into the humeral head (Vollans *et al.*, 2016). The decrease in blood flow results in a decrease in nutrients that reach the enthesis, and ultimately results in atrophy of the enthesis. The degenerative microtrauma theory then prevails, resulting in morphologies not limited to thinning and disorientation of the collagen fibers, as well as the other aforementioned characteristics. Codman ascertains that this critical region of hypovascularisation results in a disposition to a potential rotator cuff tear.

2.2.3 Tear Classification

Generally, rotator cuff tears are described as acute post-traumatic, chronic degenerative, or acute-on-chronic post-traumatic (Vollans *et al.*, 2016). An acute post-traumatic tear occurs due to a defined instance of trauma, and can incorporate mechanical means of tearing not limited to impingement or mechanical overuse. Most commonly, a tear is classified as chronic degenerative, and is due primarily to the intrinsic factors aforementioned, such as the degenerative microtrauma theory. Lastly, acute-on-chronic post-traumatic tears are augmentations of prior, existing injuries, where a mechanical overuse incident may progress an existing partial tear, to either a larger partial tear or a full tear.

Most tears involve the supraspinatus tendon or the infraspinatus tendon, and these tears are considered posterosuperior cuff tears (Vollans *et al.*, 2016). Unsurprisingly, the supraspinatus is the most common tendon that is repaired in rotator cuff surgery. This makes sense, as the supraspinatus is responsible for abduction of the arm, and thus assumes a great amount of stress. In addition, the anatomical location of the supraspinatus, passing directly inferior to the acromion process, predisposes the tendon to impingement and eventual failure. Tears are commonly classified according to the Cofield model, where less than 1 cm equates to a small

tear, 1-3 cm is a medium tear, 3-5 cm is a large tear, and greater than 5 cm is a massive tear (Vollans *et al.*, 2016). A summary of this information as well as additional classifications can be viewed in Table 1.

Table 1: Classification of Tear Sizes

Classification by tear size (Cofield)	Small	<1 cm
	Medium	1–3 cm
	Large	3–5 cm
	Massive	>5 cm
Classification by cuff tear retraction in the frontal plane (Patte)	Stage 1	Proximal stump lies close to its bony insertion
	Stage 2	Proximal stump retracted to level of the humeral head
	Stage 3	Proximal stump retracted to level of glenoid
Classification by extent of fatty muscle atrophy originally on computed tomography (CT) but now more applicable to MRI (Goutallier)	Stage 0	Normal muscle
	Stage 1	Some fatty streaks
	Stage 2	<50% fatty muscle atrophy
	Stage 3	50% fatty muscle atrophy
	Stage 4	>50% fatty muscle atrophy

It is important to classify tears as accurately as possible, as each tear needs to be treated in a way amenable to its characteristics. For instance, in the suture-anchor method of reattachment, the number of anchors and the stitching patterns unsurprisingly change according to the size of the tear. A massive tear will require a more robust attachment than a smaller tear. It is important to note that the more intrinsically a tendon is affected by degeneration, the less desirable the prognosis. That is, surgery may not be effective in repairing a torn tendon that is too degraded.

2.3 Current Treatments

Tears in the rotator cuff are identified and classified by arthrography, ultrasound and/or magnetic resonance imaging (MRI) (Gückel *et al*., 1997).

2.3.1 Surgery

Surgical methods are performed to aid in the recovery from a torn rotator cuff injury, as the goal is to minimize retear risks while preserving natural functions. This allows the patient to exit the surgery with improvement in strength and balance to the glenohumeral joint. Depending upon what goals the patient is seeking to accomplish postoperatively, surgeons can adapt their techniques of surgery. Ghodadra *et al*. stated additional factors such as the size and type of tear, tendon tissue quality, rotational inhibition, health, age and other patient demographics are all taken into consideration to determine if open, mini-open or arthroscopic surgery is a more beneficial option, as each type of surgery has both disadvantages and advantages (Ghodadra *et al*., 2009).

In order to operate on the shoulder, the patient is seated in the upright position at approximately 60 degrees. This position allows the surgeon and their medical team to manipulate the joint with ease as the surgery is performed, in contrast to the patient lying down in a horizontal position on the operating table. In all surgeries three stages of tension release are performed before the tendon is sutured down into place. Neer determined it is necessary to release the torn tendon prior to reattachment because it allows for the tendon-muscle connection to mobilize, gives way to a stronger attachment site, and aids in deltoid repair if necessary (Neer, 1972). Complications such as additional tightness in the glenohumeral joint and immobilization can occur if the tendon is not released properly. Figure 2 depicts the first two major releases. The humeroscapular (anterior release) is first released from the cuff, deltoid and other minor surrounding muscles. Then, simultaneously, the coracohumeral ligament and rotator interval capsule are freed (posterior release) to limit tightening within the cuff as well as giving way for the capsule and tendon to be pulled with ease, thus determining the insertion site (Meislin, 2000). A third release of the capsule from the glenoid is only performed if there is not enough healthy tissue for reattachment in hopes to draw the cuff in a more lateral direction towards the insertion point (Favard *et al*., 2007).

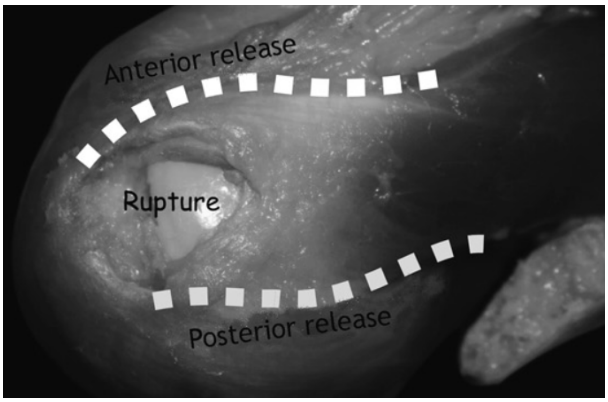

Figure 2. Primary and Secondary tendon releases prior to RCR. (Favard *et al*., 2007)

2.3.1.1 Open

As seen in Figure 3, the surgical approach to the rotator cuff is considered open when a three to six inch incision is made over the anterior superior portion of the shoulder. An incision this size is necessary for patients who have low quality tissue and tendon reduction in addition to tear sizes ranging from large (3 to 5 centimeters) to massive (greater than 5 centimeters) (Randelli *et al*., 2015). Once the subcutaneous fat layers have been separated below the surface, the deltoid muscle is separated by another three to five centimeters in order to gain unobstructed access to the joint. Through this incision, the torn tendon can be located and the attachment sites are then cleaned up by the removal of shredded soft tissue. For bone preparation, one to four anchors threaded with nonabsorbable sutures will be drilled into the humeral head. The sutures then passthrough the tendon interface three to eight times to complete the reconnection of tendon to bone. Before closing up the incision, the deltoid is reattached, also with nonabsorbable sutures. A surgery of this degree is approximately executed within an average of 100 minutes (Colvin *et al*., 2012).

Figure 3. Open RCR surgery marked with a 3-6 cm incision. (Ghodadra *et al*., 2009)

2.3.1.2 Mini Open

In contrast to the open repair approach, mini-open surgery was established in 1990 to avoid separation of the deltoid (Levy *et al*., 199). The incision size is made to be only two to four centimeters and allows for arthroscopic techniques to be used in conjunction with open repair concepts (Figure 4). The deltoid does have to be manipulated, however this is done in line with the muscle fibers, promoting a more affect recovery as compared to open RCR. Anchors and sutures are also used in this second type of surgery in efforts to reattach the torn tendon to the bone. As operational strategies have developed over the years, mini-open RCRs have influenced surgeons to limit the use of open repair techniques and sometimes complete the repair using only arthroscopic methods.

Various studies have proved that mini-open repairs for torn rotator cuffs are relatively more successful as compared to the open techniques due to a lessened strain on the surround muscles and tissues. Specifically, a study conducted by Nicholson stated, that mini-open surgeries reduce patient discomfort, provide durable results compared to open techniques, and are better suited to handle small to medium sized tears (Nicholson, 2002).

Figure 4. Mini-Open RCR surgery marked with a 2-4 cm incision. (Ghodadra *et al*., 2009)

2.3.1.3 Arthroscopic

By 2006, arthroscopic techniques were used in 58% of RCR surgeries performed due to smaller and less invasive incisions, ability for outpatient surgery, and ultimately, long term quality results (Colvin *et al*., 2012). In contrast to both open and mini-open rotator cuff surgeries, the arthroscopic approach eliminates the need for incision greater than one centimeter, displayable in Figure 5. A few small incisions are made in order to insert the arthroscope into the glenohumeral joint as well as a motorized shaver to remove any tissue fragments, a constant water stream via tubing to continuously flush out the joint, and disposable cannulas for both anchor insertion and suture passaging (Mazzocca *et al*., 2005). The camera output is on various displays in the OR to all determine the best methods for reattachment of tendon to bone. This approach is completed, on average, within 107 minutes (Colvin *et al*., 2012). Postoperatively, a significant amount of patients experience minimal pain (Bishop *et al*., 2006). However, with these benefits, there are also drawbacks to this technique. As the patient recovers, they may believe that they are able to mobilize their arm sooner than recommended, as they are not showing symptoms of pain. The tendon to bone reattachment is a slow and important process and any outside mechanical disruption could set back the recovery period. Additionally, Bishop determined that there are significantly higher failure rates for arthroscopic RCRs when the tear size is documented as large or massive, which is why the open or mini-open surgeries are more common for this tear size. No surgical technique is guaranteed, however many factors such as patient specific characteristics (age, lifestyle, intended usage of the joint), the size of the tear,

quality of the torn tissue and surrounding tissues, and location of the tear influence the choice of open, mini-open or arthroscopic surgical techniques as each repair method has advantages and disadvantages (Ghodadra *et al*., 2009).

Figure 5. Arthroscopic RCR surgery marked for device portals. (Ghodadra *et al*., 2009)

2.3.2 Materials

Currently, in each of the three types of rotator cuff surgeries, bioabsorbable or metallic anchors and nonabsorbable sutures are the main components used to aid in the reconnection of the tendon. Although the success rate of RCR surgeries are substantial, various studies have determined retear rates occur 25% to 35% of patients due to the force of the suture exerted on the tendon to bone (Cummins *et al*., 2003).

2.3.2.1 Sutures

In RCR surgeries, 0.5 millimeter diameter sutures, classified as Number 2 sutures, are used. (Abbi *et al.,* 2006). The two most used brands are Ethibond (Ethicon, Somerville, New Jersey) and FiberWire (Arthrex, Naples, Florida,), but other common brands of No. 2 sutures include Ultrabraid (Smith & Nephew, Memphis, Tennessee) and Orthocord (DePuy, Warsaw, Indiana) as determined by Bisson *et al*. (2008) and (Hurwit, *et al.,* 2014).

Ethibond sutures are composed of nonabsorbable polyester arranged in a braided structure coated in polyethylene (Najibi *et al*., 2010). This coating allows for easy knot

formation, and limits slippage as conducted in a knot evaluation experiment in an *in vitro* study (Abbi *et al*., 2006). Similarly, FiberWire's composition is a nonabsorbable polyester suture which encompasses a core of individual strands of ultra-high-molecular-weight polyethylene (UHMWPE) (Najibi *et al*., 2010). The jacket technique encompassing UHMWPE structured by Arthrex has been proven to be twice as strong compared to Ethicon Ethibond suture in both the (Abbi *et al.,* 2006) and Hurwit *et al* (2014) studies. For this reason, FiberWire sutures are commonly chosen to assist in RCRs over Ethibond sutures.

Ultrabraid also utilizes nonabsorbable polyethylene fibers in a braided form. Without the jacket commonly used by other companies, this suture is able to have a greater elongation capability, thus allowing for greater range of motion (Bisson, *et. al*., 2008). Orthocord combines both nonabsorbable and absorbable materials in order to implement less force on the tendon attachment over time. It is composed of an absorbable polydioxanone (PDS) core surrounded by a sleeve of UHMWPE and polyglactin 910 (Bisson, *et. al*., 2008). Although the strength of the suture is important to consider when repairing the rotator cuff, Lambrechts *et al*. determined that the FiberWire sutures can easily cut through the supraspinatus tendon, as compared to both Ethibond and Orthocord sutures (Lambrechts *et al*., 2014). From multiple studies analyzing mechanical properties of sutures, the "perfect" suture solution has not been established as the most common mode of failure, 90% determined by Cummins *et. al* in 2003, for any RCR surgery is at the tendon suture interface where the suture pulls through the tendon (Mazzocca *et al*., 2005), thus causing a retear.

2.3.2.2 Anchors

As arthroscopic surgical techniques advanced, the anchors have become a key component in the reattachment of tendon to bone. Suture anchors are screw like mechanisms that are typically made from stainless steel or titanium metals or plastics that are biocompatible with the human body. These plastics include polyetheretherketone (PEEK), bioabsorbable poly (L-lactic acid) (PLLA), or a combination of 60% bioabsorbable PLLA, 10% bioabsorbable polyglycolic acid (PGA), and 40% bioabsorbable Beta-tricalcium phosphate (Barber, *et al.,* 2008). Each anchor has a shaft length ranging between 11.56 to 15.14 millimeters and an outer diameter ranging 3.0 to 7.0 millimeters. The size ranges for surgical suture anchors are varied due to manufacturing choices based upon the demographics of a RCR patient. For example in Figure

6A and 6B, both the Kinsa (diameter of 3.4 mm) and Kinsa RC (diameter of 5.5 mm) anchors are produced by Smith and Nephew (Andover, MA) and are made from PEEK. They are created differently in order to cover a wider range of patient demographics.

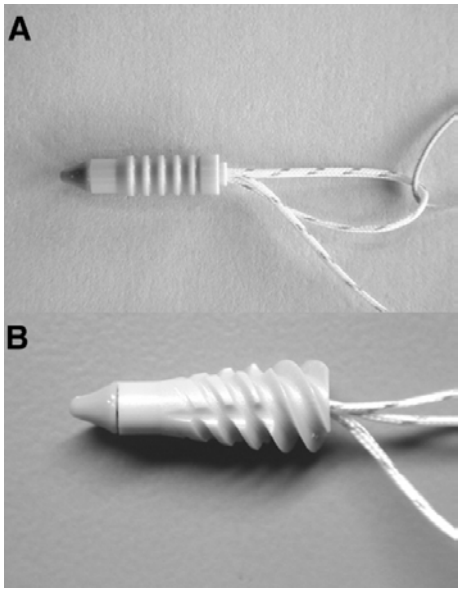

Figure 6. Kinsa (A) and Kinsa RC (B) suture anchors display variety. (Barber *et al*., 2008)

Additionally, many of these anchors have been adapted to knotless designs. In the past the anchors were also made with eyelets, allowing for the sutures to be threaded prior to implantation. However, higher stress concentrations on the eyelets due to knots caused disruption at the tendon suture interface and lead to a retear (Rhee *et al*., 2012). With the knotless design, there is less surgeon interference with the surgery because not all surgeons perform an exact protocol for all RCRs. Studies have indicated knotless anchors can withstand higher failure strengths as well (Barber *et al*., 2008). Unfortunately, with the preloaded, knotless anchors, a company's suture has to be used and it cannot be switched out in order to combine the best options for both sutures and anchors.

Instruments such as drills and awls assist with the implantation process of the anchor into the insertion site of the humeral head. Throughout RCR surgeries, the implementation of sutures anchors is more critical to the success rates of surgeries than the types of materials used for each component. Depending upon preferred surgical methods and tear characteristics, implementation

of suture anchors can be fixated in single or double row repair, as displayed in Figure 7 A-D below.

In single row RCR, the standard approach is to place three anchors linearly and 10 millimeters apart adjacent to the midpoint of the tear in efforts to minimize potential pullout. Once each anchor is in place, the suture connected to the anchor is threaded through the tendon twice, totaling 6 suture pass-through (Mazzocca *et al*., 2005). As for double row repairs, there are three variations, which include the diamond, mattress double anchor (MDA), and modified mattress double anchor (MMDA).

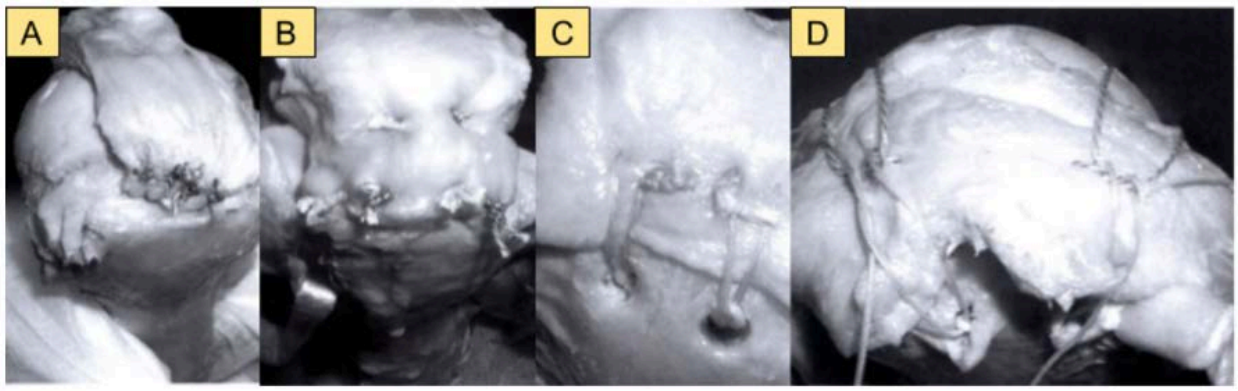

Figure 7. Single row (A), Diamond (B), MDA (C), and MMDA (D) Double row RCR. (Mazzocca *et al*., 2005)

First, the diamond repair technique has two anchors placed laterally to the tear and a third anchor placed medially to the first two. This combination of anchors allows for a total number of 8 suture pass-trough's in the tendon interface. MDA and MMDA both use four anchors, two placed parallel with the tear and two placed underneath the overhang of the torn tendon (Millett *et al*., 2004). This allows for the stress concentration to be distributed over a larger surface area, thus adjusting for potential suture pull through failure. The major difference between the MDA and MMDA is the number of tendon pass-through performed with the sutures (Gerber *et al*., 1994). The MDA technique only has four basic tendon pass-through, however the MMDA has 8. Once the basic MDA is completed with two sutures, two additional sutures are tied in horizontally in the same MDA fashion. In Mazzocca's study, each of the four techniques were analyzed and all demonstrated failure at a load greater than 250 Newtons when tested on a Materials Testing System (Eden Prairie, Minnesota). However, according to this study and

another conducted by Kim *et al*., the double row methods significantly reduced the reconstruction footprint of tear as compared to the single row methods (Kim *et al*., 2006).

2.4 Prevalence & Classification of Retears

Postoperative retears are an affliction that result in both patient discomfort and the decreased prognosis of a successive surgical repair. Retears have been shown to occur in at least 6% of patients (Mahure *et al*., 2016). This becomes significant when between 1996 and 2016, where open rotator cuff surgeries increased 34%, with arthroscopic RCR rising 600% and overall rotator cuff surgery increasing 141% (Colvin *et al*., 2012). Retears occur following surgery usually within the process of rehabilitation, when either intrinsic factors lead to an additional tear in the medial portions of the afflicted tendon or when the tendon fails to biologically heal to the humerus, resulting in the development of a physiologically weak enthesis. Critically, current surgical methods often result in repair of the affected tendon in the rotator cuff by means of scar formation rather than the regeneration of a histologically normal enthesis. Moreover, the resulting enthesis is disorganized, lacks the proper composition and structure or a histologically normal enthesis, and does not result in a tendon that transitions from unmineralized fibrocartilage to mineralized fibrocartilage and bone (Bedi *et al*., 2012). Ultimately, this is due to a lacking expression of critical cytokines that would direct the formation of the complex structure necessary for reattaching the affected tendon to the humerus in a mechanically strong way. Retears often result due to the decreased strength of the surgically mediated enthesis, and the instance rates of retears and types of retears are outlined in the proceeding sections.

2.4.1 Instance Rate of Retears

Postoperative retears can occur frequently after surgical intervention and a positive correlation exists between the size of the initial tear and the prevalence of a retear, for most surgical methodologies (J. Kim *et al*., 2014). See Figure 8 for a summary of the instance rate of retears observed in a volunteer study conducted 5 years post-surgery. Figure 8a shows the percentage of retears of various sizes (<1 centimeter, 1-3 centimeter, 3-5 centimeter, and >5 centimeter) for patients who had a rotator cuff surgery conducted using an open surgical technique. Figure 8b shows the percentage of retears of various sizes for patients who underwent

an arthroscopic knotted repair technique, and Figure 8c shows the same data for patients who underwent arthroscopic knotless repair of their rotator cuff.

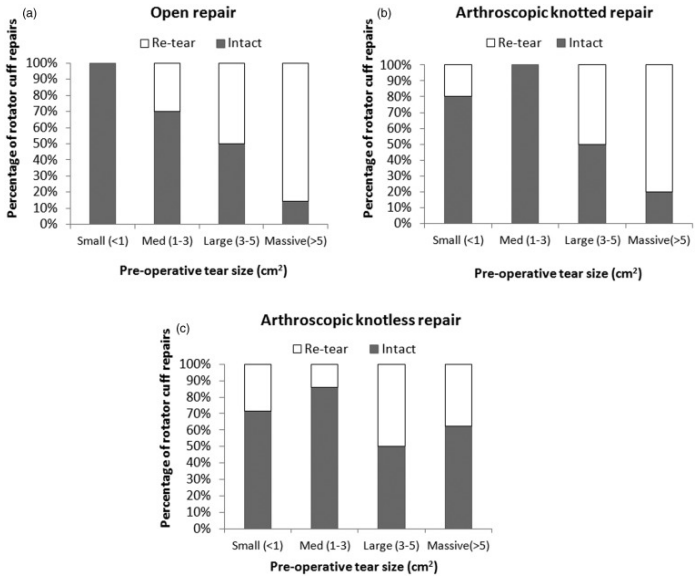

Figure 8a-8c. Instance rate of postoperative tears 5 years after surgery. (J. Kim *et al*., 2014)

Open repair and arthroscopic knotted repair surgical methodologies posed the most substantial rates of retears for large and massive initial tears. The massive retears proved the most likely to result in a retear as compared to the other tear size classifications. This was a similar trend for arthroscopic knotless repair, although the instance rate of retears was far lower compared to the alternative surgical methods. Large and massive retears pose the greatest stress levels at the suture-tendon interface, and therefore it is logical that the chances of failure would increase.

2.4.2 Types of Retears

Retears can be categorized into three classes, Type I, Type II, and Type III. Type I refers to a tendon that is unhealed, and has ruptured distally at the humeral head. A Type II retear refers to a tendon that has torn medially, relative to the tendon itself, and has resulted in a healed enthesis and a healthy reinsertion to the humeral head. Lastly, a Type III retear refers to a retear that does not fit the descriptions of Type I or II, where an example of this would be a tendon that was damaged proximally, at the muscle-tendon interface (K. Kim *et al.*, 2014). For single row

technique rotator cuff repair surgery, Type I and Type II retears occurred with rates of 71.4% and 23.8%, respectively (J. Kim *et al*., 2014). Type I retears are significantly more prevalent for the single row technique, and is similarly prevalent for the suture bridge technique. The knotless suture bridge technique reverses the trend, where 54.5% and 40.9% of the retears were Type I and Type II, respectively (J. Kim *et al*., 2014). There is distinct correlation between the type of the retear and the surgical methodology employed for the repair of the initial tear. Ultimately, a surgical fastener should aim to promote a healthy ingrowth of the tendon to the humeral head, without increasing medial stresses in the tendon. The surgical fastener used in a particular surgical methodology should influence biological healing of the tendon, and should not result in stress concentrations. In the case of a Type II retear, various intrinsic factors may be influential, and these are often not addressable with surgery. Promoting reattachment is facilitated by rotator cuff repair surgery, and thus the surgical methods should focus on mitigating Type I retears, where a mechanically strong and physiologically correct enthesis is desired.

2.4.3 Forces on the Shoulder

As previously described, the supraspinatus tendon is most often torn in rotator cuff injuries. The shoulder largely performs two functions: shoulder-abduction, performed by the deltoid and supraspinatus muscles, and shoulder-adduction performed by the teres major and laminus dorsi. In a study conducted to understand how pain affects shoulder-abduction in patients who experience chronic shoulder pain, researchers found that isometric shoulder-abduction force steadiness decreased in patients with simulated supraspinatus muscle pain (Bandholm, *et al*., 2008).

Additionally, a study was conducted in Japan by Miyamoto *et al* to understand the strain and tensile forces of the supraspinatus tendon. Ten fresh-frozen shoulder specimens were used to simulate isometric shoulder joint elevation. The supraspinatus tendon experiences large moment arm from the length of the limb. Further, the supraspinatus tendon is elongated more when elevated from -10° to 0° than above 10°. Therefore, it is more likely that a tear will occur in the supraspinatus tendon at an angle of -10° to 0° due to increased strain (Miyamoto *et al*., 2015). Unfortunately, no exact quantitative measurements are available from the study.

Further research into various forces generated by the supraspinatus tendon post tendon repair yields an additional, more helpful study, conducted by the Department of Orthopedic

Surgery at Tohoku University School of Medicine in Sendai, Japan. Using finite element models, the study simulates contraction forces in the supraspinatus tendon by exerting a tensile force on the proximal end of the tendon. Experiment groups include a single-row fixation, double-row fixation and transosseous suture fixation of the supraspinatus tendon (Sano *et al*., 2007).

A popular method for RCR is an arthroscopic procedure using suture anchors, namely because it is minimally invasive and allows for the preservation of the deltoid muscle origin. However, the re-rupture rate of this procedure when applied to large to massive sized tears is higher than that for conventional transosseous suture repair (Black *et al*., 2016). The results indicate that both the single-row and double-row fixations exhibited a higher stress concentration within the tendon than that for the transosseous suture method. According to the Finite Element (FE) models, stress concentration in the single and double-row fixations extended from the suture anchor site up to the bursal surface of the tendon. The abduction angle of the shoulder joint was set at 0° and the tendons' thickness was set as 21.9 millimeter, corresponding to the average supraspinatus width. In order to model the system using FE models, some assumptions were made including defining a 0.025 millimeter-wide gap between tendon and bone based solely on technical, not physiological, reasons. Further, the humeral head and supraspinatus tendon were considered isotropic materials, meaning that they exhibit the same material properties along all axes. Limitations of this study include that the study does not reflect dynamic data regarding shoulder abduction and that the study purely shows the stress concentrations where mechanical failure is likely to occur, not where it actually occurs (Sano *et al*., 2007).

2.5 Patent Review

As stated, the client for this project, Dr. Robert J. Meislin, currently has two patents on both the concept and methods for surgical RCR with a hook-and-loop fastener. These documents were initially the guidelines for the preliminary prototypes that were created, as the team was tasked with "attaching the tendon or ligament to a boney structure or to another tendon or ligament portion." However, as various iterations were developed, the team veered away from a hook-and-loop fastener concept, thus developing a novel and innovative device. (Meislin, 1999) and (Meislin, 2000).

2.6 Technical Components

Knowledge of a variety of cutting edge tools will be beneficial to the project outcome. Software components including Computer Aided Drafting and 3D printing software are integral in designing prototypes. Further, computerized analysis of the integrity of said prototypes can eliminate monetary and material waste. Finally, there are many options available for 3D printing prototypes, within the Biomedical Engineering department, WPI, and the greater online and global industrial community.

2.6.1 Software

SolidWORKS is a Computer Aided Drafting (CAD) software that allows for rapid prototyping of various component parts and assemblies. By converting a SolidWORKS CAD file into a stl file, a 3D print can be then generated by converting the .stl file into a .x3g file. In depth knowledge on the functionality of SolidWORKS is provided to the team by Emily Viloudaki based background knowledge and skills gained from course, Engineering Science 1200. Additional software under consideration includes sli3er, a G code generator, and Simplify 3D, a 3D printing slicing software. Notably, both softwares allow for additional parameter settings within the .x3g file conversion process. In particular, sli3er is an open source, free software, with the capability to print with multiple extruders, adjust layer heights and infill densities. It also allows the user to include a cooling function in order to allow the material to cool rapidly after extrusion, based both on extrusion speed and fan cycling (Bell, 2014). However, it is yet to be seen if the Qidi printer is capable of handling such detailed specifications.

2.6.2 Finite Element Analysis

Finite Element Analysis (FEA) is method by which computers can analyze how a part will react to physical forces including heat and material wear-and-tear. Essentially, FEA will show how a product will break, and how it will work compared to how its operation was expected. By employing FEA, users can significantly reduce rework times and costs (Akin, 2010). Given that the project is subject to budgetary and time constraints, using FEA will be particularly beneficial. Some properties of interest regarding FEA include understanding how temperatures, forces and pressures affect the part in question. FEA works by generating discrete geometries from the conglomerate part. Further, plane stress and strain can be further simplified

using 2D assumptions. One of the main uses of FEA is to model the behavior of structural beams. Nonlinear stress analysis of interest to the project in order to determine the impact of strain hardening in the complex load deformation relationship of plastic materials. As a general rule, shell mesh is generated to model surfaces and beam elements are generated to model structural members of the part (Akin, 2010).

2.6.3 3D Printing Technology

It is important to note that 3D printing encompasses a variety of solid freeform fabrication (SFF) technologies (Chia *et al*., 2015). The 3D printer provided to the team is a Qidi 3D Printer that comes equipped with a MakerWare software installation. Qidi printers use fused deposition modeling (FDM) machines that utilize an additive manufacturing process. The printer is capable of printing PLA and ABS; however, ABS will not be used for the purposes of this project because it is not biocompatible. The Qidi printer operates by printing an .x3g file from an SD card inserted into the printer. The Qidi printer has two extruders, a left and right, and has a heated build plate. Further, a cooling fan operates to keep the machine from overheating. Accompanying the printer hardware and software is a setup and user manual, both of which were read thoroughly. The printer was successfully assembled, performed troubleshooting and tested throughout multiple prototype prints.

In contrast to ABS, PLA is biocompatible and treated and can offer a number of additional beneficial qualities. For example, PLA has a tight tolerance control and can be dried in an oven to prevent deformation caused by drying in a moist environment. (PLA for 3D printing 2015). An untreated PLA filament is hygroscopic, meaning that the material will absorb moisture from the air, causing it to swell. However, the Bioplastics Division of Teknor Apex have developed a modified version of PLA named Terraloy 3D-40040 that has more desirable properties. The Terraloy compound sits at the intersection of 3D printing and bioplastics. Benefits include a twofold increase in heat distortion temperature (HDT) and a four-fold increase in impact strength over untreated PLA resins (Products in the news: High-heat and -impact PLA for 3D printing yields tight tolerances and less shrinkage and.2015).

Additional research into other printing technologies was conducted. The optimal printing temperature for PLA on a Deltabot printer ranges from 195 - 215 °C. The study indicates that the surface roughness of the printed part is directly proportional to the printing speed. Additionally,

WPI houses a number of 3D printers available to the student body at a cost. One such machine is the Objet machine. Unfortunately, this machine only prints using one biocompatible material, although it yields a much higher resolution than the Qidi machine “Stults (2016, Personal Communications). According to industry research, there are eight variations of the Objet PolyJet System. It appears that of these eight machines, three are able to print with MED610. MED610 is the only tested biocompatible material that is readily available in the (print) lab on the WPI main campus, and for ease of usage and budgeting constraints, this material was deemed to be ideal for the project. These machines include, the OBJET30 PRIME, the OBJET EDEN260VS, and the OBJET260/350/500 CONNEX3 (Reichl *et al.*, 2016). Given the product catalogue for these machines, no other biocompatible materials are available for 3D printing in the Objet.

There are many challenges presented by the 3D printing of biomaterials. For one, the architectures of the printed material influences the structure of the tissue that grows upon a 3D printed scaffold. Architectural features of the material include pore size, shape, porosity, spatial distribution and pore interconnection. Many surface modifications can be completed after printing. Finally, the 3D printing industry has developed to refine resolutions for industrial applications, however, these advancements do not directly translate to the SFF of biomaterials (Chia *et al*., 2015)

2.6.4 Biomaterials

A biomaterial is a material that can interface with the human body for a specified amount of time without yielding significant adverse events (ISO, 2016). Depending on the duration and level of contact, biomaterials can be of varying degrees. Further biomaterials under investigation are silk and nylon, in addition to poly(lactic) acid and PolyJet photopolymer.

2.6.5 Polylactic Acid (PLA)

PLA is one of the most common commercially available biomaterials and has been approved by the FDA for applicational use in many humans (Araque-Monrós *et al*., 2013). PLA is classified as a synthetic semi-crystalline material (Cordewener *et al*., 2000). Commonly used to reinforce mechanical properties of gels, PLA exhibits stronger mechanical properties than fibrin (Gundy *et al*., 2008). A study indicates that the PLA remains intact and stable after a 36 week incubation period. Indicators of stability include pH test results and Instron 5544 pull

testing results regarding tensile strength. Interestingly, the molecular weight of the PLA decreased by 6% during the 36-week incubation. Accelerated degradation profiles of PLA can be extrapolated to replicate long-term *in vivo* degradation when the PLA undergoes accelerated hydrolysis at 90° C (Gundy *et al*., 2008). Further, depending on the molecular weight and distribution of the PLA molecule, the degradation extracts can affect the pH and osmolarity of cell cultures, causing cytotoxicity (Cordewener *et al*., 2000).

A "regenerative prosthesis" uses a hollow, braid-like structure composed of PLA and an outer surface non-adherent coating to characterize tendons and ligaments. Tendons join muscles to bones and ligaments join bones to bones. The design has a Young's modulus of 1370 ± 90 megapascals which decreases by a factor of 4 over 12 months, indicating that it degrades over time. L929 fibroblasts from passage 8 were cultured inside the hollow interior of the PLA braid for 14 days, displaying biocompatibility. Actin cytoskeletal staining of the cells in conjunction with confocal scanning microscopy with an inverted laser was used to assess cell distribution and adhesion. The braid dimensions and characteristics, including number of threads and braiding angle, can be adjusted to adapt the "regenerative prosthesis" to various tendon and ligament applications. Tensile properties were characterized using stress-strain and dynamic tests at room temperature (Araque-Monrós *et al*., 2013).

2.6.6 PolyJet Photopolymer (MED610: Proprietary Formulation)

This material is the bio-compatible PolyJet Photopolymer (MED610). The printed final product is colorless, transparent, and rigid. Biocompatibility tests in accordance with ISO 10993-1:2009 have already been conducted, indicating that the material satisfies requirements outlined for prolonged skin contact of more than 30 days. However, MED610 is only approved for mucosal-membrane contact for less than 24 hours and not approved for implantable devices. Additionally, the MED610 fabrication boast easy support removal, allowing for more detailed component creation through the use of removable support material (Bell, 2014). Unfortunately, the exact chemical components of the MED610 material are not available because of proprietary information.

2.7 Bioadhesives

Bioadhesives are an alternative method for achieving tendon to bone adhesion after implementation of device. The team wanted to completely remove all need for suture anchors and sutures to help treat all RCR surgeries. The team pivoted to use mussel adhesive but was not available in the market yet. The team then decided to use adhesives that are easily used in the market such as, ethyl cyanoacrylate, polyurethane adhesives, and Vetbond tissue adhesive.

Ethyl cyanoacrylate is a non-toxic, colorless, fast- acting adhesive, it can hold up to 2,000 lbs. per square inch (Roger, 1999). A given catalyst is required to activate this formula. This catalyst can be water, which is commonly found in any surface. Polyurethane adhesive has industrial holding power and versatility. The water activated polyurethane formula expands into materials to form an incredibly strong bond to virtually anything (Lutz Tool Company, 1999). This chemical formula is 100% waterproof glue, and strong enough to stand up to the elements. Plus, its expansion allows it to penetrate the glued surface for a superior bond. Vetbond formula is known to be a tissue adhesive produced by 3M. Vetbond quickly and conveniently closes minor wounds, often eliminating the need for sutures and/or bandages (Thulin, 1979). It is most commonly used in veterinary applications, thus looking at the utility of the device it could be used for veterinary application, and thus this adhesive would work in collaboration with animal use. All in all, the need for bioadhesives is needed to remove all use of suture anchors and sutures to attach tendon to bone. Further investigation of this will be done in the report, to examine if it is a viable option to pursue for final prototype development.

2.8 Food & Drug Administration Regulations

The Food and Drug Administration (FDA) is the major governing body in the United States that works to ensure the public's health. Areas that this entity regulates include human drugs, biological products and medical devices (*Fda*2014). There are a variety of regulations that pertain to the design project from many entities, including the International Standards Organization and the American Society for Testing and Materials (ASTM).

2.8.1 International Standards Organization (ISO)

Closely aligned with the FDA are a number of International Standards Organization (ISO) regulations. One such regulations is ISO10993-1:2009. Biological Evaluation of Medical

Devices – Part 1: Evaluation and Testing Within a Risk Management Process. ISO10993-1 endeavors to ensure that no unacceptable adverse biological responses result from bodily contact with the device or its component materials. The regulation categorizes devices based on the nature of body contact. Categories include surface device, external communicating device, and implant device. Further, the duration of contact is also a major factor in determining what kinds of testing must be performed. Contact durations include three levels: A, B, and C as limited, prolonged, and permanent, respectively. A variety of tests are either required or recommended in order to ensure satisfactory compliance. These tests include, cytotoxicity, sensitization, and irritation among others (ISO, 2016). The standard also includes outlines for test methods and test reports. For example, the test parameters, acceptance criteria, results analysis, and conclusions should be included in the test report. Existing market data may also be used to substantiate biocompatibility claims. (ISO, 2016).

Another standard to be considered is ISO11737-2:2009, Sterilization of Medical Devices: Microbiological methods – Part 2: Tests of sterility performed in the definition, validation and maintenance of a sterilization process. The most common sterilization methods include autoclaving and ethylene oxide exposure. Any device that is used during a surgical operation must satisfy sterilization requirements (ISO, 2006).

2.8.2 American Society for Testing Materials (ASTM)

The American Society for Testing and Materials (ASTM) outlines a variety of testing standards that relate to the project. They include but are not limited to the following standards (International Symposium on Engine Coolant Technology, ASTM Standards and Engineering Digital Library, & ASTM International, 2004):

- ASTM F 2847-10: Standard Practice for Reporting and Assessment of Residues on Single Use Implants
- ASTM WK32535 (2011). New Practice for Establishing Limit Values for Residues on Single Use Implants.
- ASTM E691 – 15. Standard Practice for Conducting an Interlaboratory Study to Determine the Precision of a Test Method
- ASTM D638-14. Standard Test Method for Tensile Properties of Plastics

Although ASTM, ISO and the Food and Drug Administration (FDA) are separate governing bodies, knowledge of the variety of regulations and standards as they apply to medical devices will help guide the design process.

2.9 Cost Analysis

The average cost of medical per patient undergoing rotator cuff repair surgery is $50,302.25 (Savoie *et al*., 1995). Another study investigates the cost savings of anchorless arthroscopic double-row repair compared to double-row anchored (TOE) repair. The implant cost for TOE repairs was on average $1,014.10, with massive tears costing up to $1,500. (Black *et al*., 2016) In comparison, anchorless repair implants cost on average $678.05 with massive tears pricing up to $716. Interestingly, there was no significant difference in average total operative time between the TOE and anchorless groups, taking 99 and 98 minutes, respectively. (Black *et al*., 2016). These calculations do not include prices for motorized shavers, suture passers, or surgical instruments already owned and supplied by the hospital. Additional costs to the patient, including diagnosis, hospital stay, pain medication, physical therapy and other healthcare related costs are not considered. Overall, arthroscopic transosseous rotator cuff repair surgery offers significant cost savings over TOE repairs.

The instance of RCR surgeries is becoming increasingly common. For example, in 2006, an estimated 98 procedures were performed per 100,000 people in the U.S., and now there is an estimated 250,000 repairs in recent years. (Black *et al*., 2016). Further, the study showed that double row repair is not cost effective in any tear-size range.

3 PROJECT STRATEGY

A project strategy was created to design a biological surgical fastener for the use of rotator cuff repair surgery in order to meet the stakeholders' needs. Necessary steps toward creating, implementing, and testing a successful design were established. The client statement was reviewed in order to research the current solutions. Through group and advisor meetings, the initial client statement was revised to fit the final goal of this project. A basic outline of tasks was completed to keep the project on schedule throughout this academic year.

3.1 Initial and Revised Client Statement

The initial client statement was taken directly from literature provided to us by the advisor. The text follows and is indicated in quotes.

"Currently, tendon tears in the shoulder are typically repaired with suture anchors placed in the bone. Sutures are then passed through the torn tendon and tied down to the bone. This creates a "spot welding" approach. The hook and loop structure of the commercially available "Velcro" adhesive is the basis for the project; in this case to create a biological absorbable solution. This project is therefore intended to adopt this technology to develop an easy "fastener" system for use in various surgical applications. You are expected to create at least one functioning prototype for at least one of the many possible surgical applications for the device. At the end of the project, you should be able to demonstrate the utility of the device in the application area(s) they have chosen at the beginning of the project. Ideally, they should demonstrate the use of the device in an appropriate "model system." Sufficient numbers of prototypes should be tested (For statistical significance) to calculate the stress-strain curve and "strain-to-failure." The students should follow the engineering standards guidelines in the design process and the analysis of the materials and the device with particular focus on the materials property and FDA regulations for an implantable device."

This initial client statement was very broad and has a wide scope for the project. In order to outline achievable deliverables, the team consolidated this initial client statement into its first revision. The first revised client statement was;

"Create bio-absorbable, Velcro-like device to replace sutures and anchors in rotator cuff repair surgeries. Develop prototypes, demonstrate use in a model system, follow FDA regulations, and perform statistical analysis."

A second revision of the client statement was prompted by communication with the sponsor. After speaking to Dr. Meislin over the phone, it became apparent that the target patients suffer large to massive RC tears and the goal is to foster reattachment of the tendon to the bone by any means possible, whether this incorporates a Velcro-like structure or not. The second and final revised client statement was;

"Develop a device to reattach the affected tendon into its insertion point in patients undergoing large to massive RCR surgeries such that the instance rates of Type I retear rates are minimized. Several prototypes will be developed and the final design will be selected based upon mechanical and biocompatibility testing results."

The team realizes that the client statement may continue to evolve over time. Therefore, the scope of the project is not yet permanently defined, however, the team is exploring a variety of options to keep an open mind.

3.2 Objectives

Based on the information gathered from the initial client statement as well as multiple meetings with Dr. Meislin, the objective of the project is as follows: develop a way to ensure proper ingrowth of the affected tendon into its respective insertion point in patients undergoing large to massive rotator cuff repair surgeries such that the instance rate of Type I retear rates is minimized. Since a correlation exists between the type of surgical fastener used and the instance rate of Type I retears, the final design aims to develop a novel surgical fastener that promotes biological healing of a physiologically normal enthesis at the tendon-bone interface in RCR

surgeries. It is imperative that all potential materials are analyzed for biocompatibility as this device must have a degradation rate no less than nine months. Any chosen material may need modification in order to adapt well to the surgical site. For instance, the density of the material of the device may be changed to alter its properties such as stiffness, such that it can conform to the anatomy of the glenohumeral joint. Any material modification will need testing to insure biocompatibility and thus conformity to FDA regulations.

Through the development of the client statement, the team established the following objectives that were preliminarily ranked according to significance using a pairwise comparison chart.

1. Decrease patient discomfort: The surgical fastener must ensure a normal healing process that does not increase the patient's experienced pain. In addition, the fastener should facilitate a swift healing process such that the patient can regain function of their affected arm.
2. Adapt device to different size tears: Rotator cuff tears are categorized based on their size, where a small tear is characterized by separation of less than 1 centimeter, a medium is between 1 and 3 centimeters, a large is 3 to 5 centimeters, and a massive tear is greater than 5 centimeters or separation (Vollans *et al.*, 2016).
3. Attach tendon-to-bone: Rotator cuff repair surgery involves the reattachment of a severed tendon (usually the supraspinatus) to the humeral head in an effort to promote biological healing and reinsertion of the tendon into the bone. Currently, anchors are inserted into the bone and serve as attachment points for sutures that are sewn through the tendon such that when pulled tight, the tendon is held in place so biological healing can occur. The design must be able to support this attachment and be able to withstand the mechanical forces of the glenohumeral joint.
4. Ensure biological and mechanical integrity: The rotator cuff is highly dynamic and is subjected to mechanical forces in varying directions based on the affected tendon. In the case of the supraspinatus, it supports the abduction of the arm, and is therefore subjected to high amounts of mechanical stress, especially if the patient is carrying a payload while abducting their arm. In addition, the glenohumeral joint is internal, and is surrounding by various fluids, including synovial fluid, which may react with a surgical fastener. Any design created must be able to withstand the mechanical and chemical environment of the

glenohumeral joint, such that the device does not fail mechanically or react adversely with the body.

5. Promote cell migration: After contacting the project's sponsor, Dr. Meislin, there was apparent interest in the developed device promoting cell migration from the tendon to the insertion site on the humerus, such that a physiologically normal enthesis can be formed readily due to biological healing. Dr. Meislin is interested in incorporating a cellular scaffold into the design, so that the healing process may be expedited and potentially improved.
6. Adhere to FDA regulations: Any device created for implantation must meet FDA regulations, specifically those regarding biocompatibility.
7. Target large-massive sized tears: Dr. Meislin suggested an interest in targeting large-massive sized tears, claiming that the current suture-anchor method is adequate with addressing small and medium sized tears.
8. Use successful bioadhesive: Attaching any developed device to both soft and hard tissues is integral to a successful design. A bioadhesive such as mollusk glue or crosslinked fibrin glue may be necessary to ensure that the device remains fixed in place for the entire healing process.
9. Design for arthroscopic delivery: Currently, most RCR surgeries are performed arthroscopically and the currently accepted suture-anchor method is easily performed with such methodology. In order to prevent drastic alterations to the surgical methodology incorporated during RCR surgery, any design developed should be easily delivered with a traditional arthroscope.
10. Use Velcro-like concept: The client, Dr. Meislin, currently has a patent (#US6039741) outlining a methodology that incorporates the hook and loop structure of commercially available Velcro. Incorporating this idea is protected by the patent and should be easily incorporated.
11. Apply to other surgeries: The patent outlining the methodology for developing an alternative surgical fastener uses the rotator cuff as a model. The client suggests developing a surgical fastener that can be adapted to other types of surgery, such as ACL reconstruction surgery or gastric bypass surgery.

All of the aforementioned objectives were compared against each other in the following pairwise comparison chart such that a -1 indicates the objective in the left column was deemed more important than the objective in the top row, a 0 indicates equal importance, and a 1 indicates greater importance of the objective in the top row.

Table 2: Initial Pairwise Comparison Chart

	Attach T->B	Size: Large/Massive	Velcro Concept	Arthroscopic Delivery	Bioabs/ Mech Integral	Cell Migration	Bioadhesive	Other Apps	Patient Discomfort	Adaptable (diff tears)	FDA Regs
Attach T->B	0	0	-1	-1	0	-1	0	-1	0	0	0
Size: Large/Massive	0	0	-1	-1	0	0	1	-1	1	0	0
Velcro Concept	1	1	0	1	1	1	0	-1	1	1	0
Arthroscopic Delivery	1	1	-1	0	1	1	1	0	0	1	0
Bioabs/ Mech Integral	0	0	-1	-1	0	0	0	-1	0	0	0
Cell Migration	1	0	-1	-1	0	0	-1	-1	0	1	0
Bioadhesive	0	-1	0	-1	0	1	0	0	1	1	0
Other Apps	1	1	1	0	1	1	0	0	1	1	1
Patient Discomfort	0	-1	-1	0	0	0	-1	-1	0	-1	0
Adaptable (diff tears)	0	0	-1	-1	0	-1	-1	-1	1	0	0
FDA Regs	0	0	0	0	0	0	0	-1	0	0	0
TOTAL:	4	1	-6	-5	3	2	-1	-8	5	4	1

After acknowledging other stakeholders' opinions for the primary objectives, the team reduced necessary objectives to six categories; mechanical compatibility of the device, ensure it will not inhibit cell growth, biocompatibility, integrations with current surgical techniques, reattach tendon to bone, and be adjustable for large to massive tear sizes. Table 3 displays a secondary pairwise comparison with 0 representing the top row objective is less important than the left column objective, 0.5 representing they're equal and 1 representing the top row objective is more important than the left column objective.

Table 3: Pairwise Comparison Chart

	Mech. Integ	Doesn't Inhibit Cell Growth	Biocompat	Easy of use with Current Approach	Tendon to Bone	3 - 5< Sizes Adj
Mech. Integ		0	0.5	0	0.5	0.5
Doesn't Inhibit Cell Growth	1		1	0.5	1	0.5
Biocompat	0.5	0.5		0	1	0
Easy of use with Current Approach	1	0.5	1		1	1
Tendon to Bone	0.5	0	0.5	0		0
3 - 5< Sizes Adj	1	0	0.5	0	1	
Totals	4	1	3.5	0.5	4.5	2

The new design objectives for this project are as followed:

1. Device should attach tendon-to-bone in the rotator cuff
2. Ensure the mechanical compatibility with the shoulder
3. Device must be biocompatible
4. Adapt device to different size tears within large to massive tear range
5. Should not inhibit cell migration or blood flow
6. Compatible with current surgical techniques and instruments

3.3 Design Constraints

Four major constraints were identified during the inception of the objectives for the project. All of the constraints relate to the creation of an alternative surgical fastener using 3D printing as the primary manufacturing method.

Printing Capabilities: The device will be manufactured using a 3D printer. Students have full access to a Qidi 3D printer but have only been given two printing materials, which are PLA and ABS. Ultimately, the available 3D printer can only print with one biomaterial, and if any other biomaterials are to be tested, the printing of the design will need to be outsourced. In addition, the resolution of the 3D printer is limited by the size of the nozzle on the extruder and the precision with which the carriage can be moved by its motors. If the design is to incorporate a higher resolution than the available printer can print design will have to be outsourced. Another available option is the Rapid prototyping lab on campus where the 3D printers available for student's use is Dimension SST 1200es, Objet260 Connex, and the Markforged Mark Two. These machines are meant to be used for parts that cannot be easily purchased or produced using other on-campus resources. That lab has access to more printing materials and higher resolution than the ones given to us, such as MED610 which is biocompatible. If this material does not fulfill the needs for the design it will need to be outsourced, which could impact the timeline of the project as well as the budget constraints. The client statement suggested the use of a 3D printer for designs. However, the team does not want to be held back on the limitations of the 3D printer to make a scaffold. Therefore, other ways of building a scaffold were taken into consideration such as electrospinning scaffolds.

Limitations of Testing: The device must be able to be tested using an appropriate model system. Such testing would be based on an *in vitro* environment compared to *in vivo,* which may not actually be an accurate representation of the *in vivo* environment of the rotator cuff. A method for consistent mechanical testing of all the designs is also important. If each design is tested using, for instance, a different method for loading the sample into the Instron structural testing machine, each test will be inherently different and produce results that cannot accurately be compared against one another. Therefore, developing a consistent testing model will be paramount to the project's success.

Time Frame: The device must be designed and tested within the 2016-2017 academic school year. In order to do this, students must meet all of the client's needs and successfully have a working prototype by the end of the year. Therefore, it will be important to ensure proper communication and scheduling with all stakeholders to ensure everyone's goals are met.

Limited Budget: The development costs of the device must adhere to a fairly limited budget of $1,000. Efficient use of time and materials will be especially important.

3.4 Project Approach

The intention of this project is the development of various designs and the selection of a final working prototype based upon qualifications. A Gantt chart and work breakdown structure were implemented into the design process to ensure the project stays on schedule and all goals were completed. In Figure 9, the Gantt chart specifically structures the deadlines for the project. Each task is associated with an expected completion date in order to meet the required criteria of the subsequent goal. As for the work breakdown structure, Figure 10, shows a method to organize deliverables by further developing detailed tasks. By communicating the design process with the client and advisor, changes to the overall project will be implemented with ease.

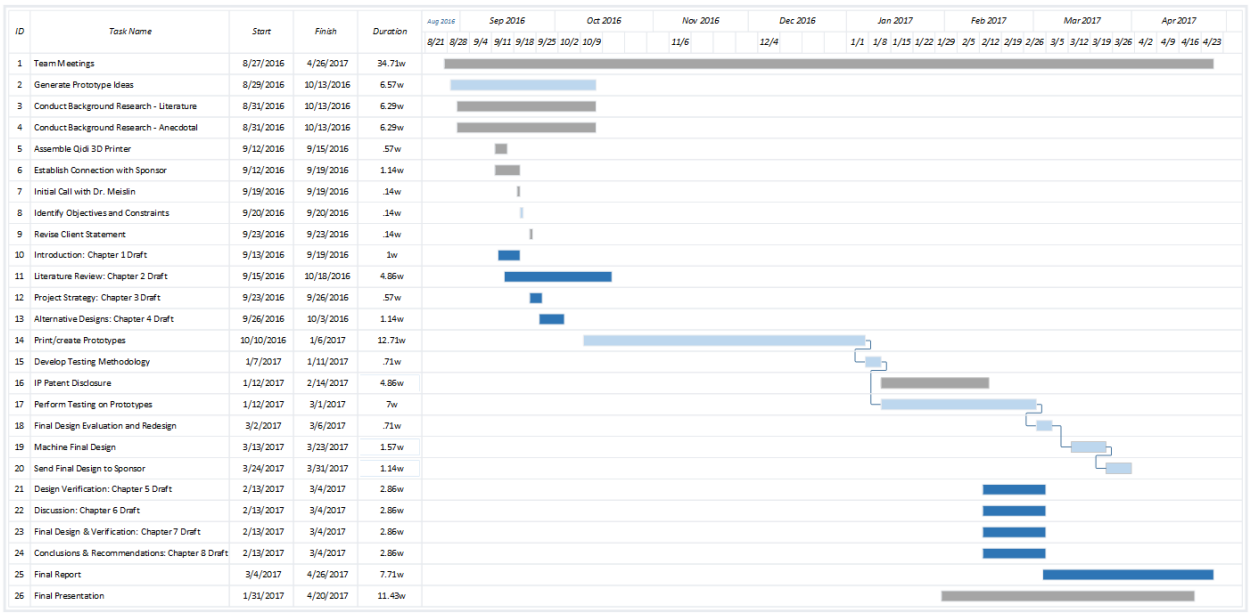

ID	Task Name	Start	Finish	Duration
1	Team Meetings	8/27/2016	4/26/2017	34.71w
2	Generate Prototype Ideas	8/29/2016	10/13/2016	6.57w
3	Conduct Background Research - Literature	8/31/2016	10/13/2016	6.29w
4	Conduct Background Research - Anecdotal	8/31/2016	10/13/2016	6.29w
5	Assemble Qidi 3D Printer	9/12/2016	9/15/2016	.57w
6	Establish Connection with Sponsor	9/12/2016	9/19/2016	1.14w
7	Initial Call with Dr. Meislin	9/19/2016	9/19/2016	.14w
8	Identify Objectives and Constraints	9/20/2016	9/20/2016	.14w
9	Revise Client Statement	9/23/2016	9/23/2016	.14w
10	Introduction: Chapter 1 Draft	9/13/2016	9/19/2016	1w
11	Literature Review: Chapter 2 Draft	9/15/2016	10/18/2016	4.86w
12	Project Strategy: Chapter 3 Draft	9/23/2016	9/26/2016	.57w
13	Alternative Designs: Chapter 4 Draft	9/26/2016	10/3/2016	1.14w
14	Print/create Prototypes	10/10/2016	1/6/2017	12.71w
15	Develop Testing Methodology	1/7/2017	1/11/2017	.71w
16	IP Patent Disclosure	1/12/2017	2/14/2017	4.86w
17	Perform Testing on Prototypes	1/12/2017	3/1/2017	7w
18	Final Design Evaluation and Redesign	3/2/2017	3/6/2017	.71w
19	Machine Final Design	3/13/2017	3/23/2017	1.57w
20	Send Final Design to Sponsor	3/24/2017	3/31/2017	1.14w
21	Design Verification: Chapter 5 Draft	2/13/2017	3/4/2017	2.86w
22	Discussion: Chapter 6 Draft	2/13/2017	3/4/2017	2.86w
23	Final Design & Verification: Chapter 7 Draft	2/13/2017	3/4/2017	2.86w
24	Conclusions & Recommendations: Chapter 8 Draft	2/13/2017	3/4/2017	2.86w
25	Final Report	3/4/2017	4/26/2017	7.71w
26	Final Presentation	1/31/2017	4/20/2017	11.43w

Figure 9. Gantt Chart for Design Process.

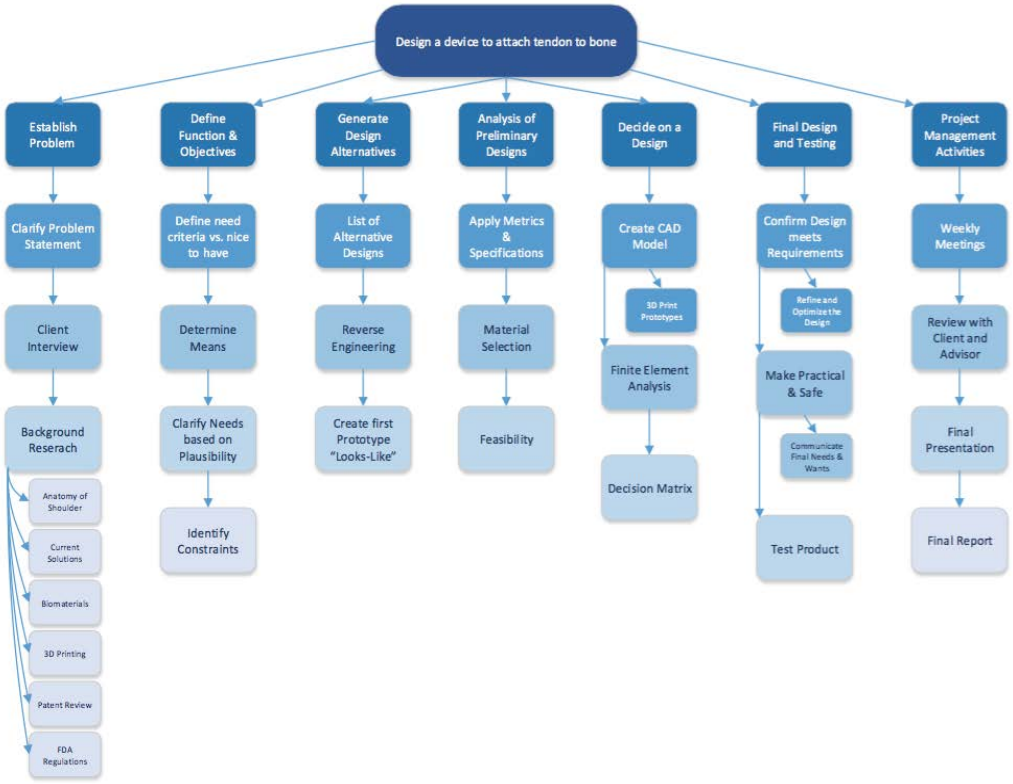

Figure 10. Work Breakdown Structure of Design Process.

After being tasked to design a device to aid in the reattachment of tendon to bone in rotator cuff surgeries, the problem statement was clarified and broken down. A preliminary client interview was conducted, and from there, a revised statement was drafted. Further research was completed relating to the anatomy of the shoulder, current treatment options for torn rotator cuffs, biomaterials to consider, 3D printing details, patent review and Food and Drug Administration Regulations. Once the research was conducted, a key list of functions was compiled to prove the device was novel. Objectives for the device were analyzed using a pairwise comparison chart in order to significantly rank them. Throughout the year, these functions and objectives were constantly referred to as the foundation for this project. Additionally, to keep the design plausible, a compilation of constraints was established. During this process, it is imperative that there are no limiting factors or negative opinions when drafting prototypes, thus allowing for unrestricted design. Various schematics were created and then rated based on the previously identified constraints. Preliminary "looks-like" models were developed first in order to gain a deeper understanding of other future designs.

As each design was developed, the determined functions, objectives and constraints were used to analytically determine which ones were worth pursuing in greater detail. It is important to apply metrics to the designs based on costs, materials, and regulations. With this first design screening, larger complications can be avoided. With further design analysis completed by using a comparative matrix, a select few designs were prototyped using CAD software and then developed using a 3D printer. Theses designs encompassed the highest-ranking functions and objectives, as determined by the pairwise comparison chart. As the creation process continued, secondary plans were also determined if unfortunate circumstances occurred. Each device was subjected to mechanical testing, biocompatibility analysis in an *in vitro* setting, and with the client in order to complete a Finite Element analysis. From there a final prototype was chosen and redesigned based upon final discussions with all stakeholders.

Throughout the design process, documentation of any ideas, prototypes, tests, and analyses were accurately completed for incorporation into the final presentation and report. Before finalizing all deliverables, client and advisor approval was obtained to ensure the device m*et al*l necessary requirements.

3.5 Engineering Standards

The design requirements for the project encompass adherence to ISO and ASTM standards. Ethical laws will be followed and safety regulations taken into consideration.

3.5.1 ISO and ASTM Standards

Given that the device will be implanted during surgery, there are a number of standards and specifications that we must satisfy. The paragraphs below introduce the standards and express how the project's approach will satisfy the requirement.

ISO10993-1:2009. Biological Evaluation of Medical Devices – Part 1: Evaluation and Testing within a Risk Management Process.: The device will come into direct contact with the human body. This standard must be followed to ensure that no unacceptable adverse biological response results from bodily contact with the device's component materials. Based on the Evaluation Endpoints for Consideration table included in the standard, the device will be considered a "C," permanent, implant that directly contacts tissue/bone (ISO, 2016). The resulting recommended ISO tests are:

- Cytotoxicity
- Sensitization
- Irritation or Intracutaneous Reactivity
- Acute Systemic Toxicity
- Subacute/ Subchronic Toxicity
- Genotoxicity
- Implantation

The additional FDA recommended endpoint tests are:

- Material-mediated pyrogenicity
- Chronic Toxicity
- Carcinogenicity

All non-preliminary tests should be compiled into test reports. The reports should include test article preparation, preferably of the final product. A test method should also be included and

will be derived from FDA documented recommendations. Finally, the test parameters, acceptance criteria, results analysis, and conclusions should be included in the test report. Existing market data may also be used to substantiate biocompatibility claims. (ISO 10993-1, 2009).

ISO11737-2:2009, Sterilization of Medical Devices – Microbiological methods – Part 2: Tests of sterility performed in the definition, validation and maintenance of a sterilization process: 1. The device must be properly sterilized before implantation to ensure minimal risk of infection to the patient 2: Various sterilization methods include autoclaving and ethylene oxide exposure will be considered for use. However, the final decision is contingent on the material properties of the final material selection. After the material is selected, the sterilization processes can be developed.

ASTM Testing standards: There are a variety of applicable ASTM testing standards that relate to the project (*ASTM designation*). They include but are not limited to the following standards:

- ASTM F 2847-10: Standard Practice for Reporting and Assessment of Residues on Single Use Implants
- ASTM WK32535 (2011). New Practice for Establishing Limit Values for Residues on Single Use Implants.
- ASTM E691 – 15. Standard Practice for Conducting an Interlaboratory Study to Determine the Precision of a Test Method

Additional standards on the pull-testing parameters based on the geometries of the selected designs will be investigated and followed.

3.5.2 Risk Assessment for Safety

As always, safety is paramount to the success of any design. The risk assessment included in ISO 10993 indicates that devices posing risks such as adverse systemic or local effects, cancer and/or adverse reproductive/developmental effects must be carefully evaluated. These risks are only acceptable if the benefits of using the device outweigh the associated risks.

A risk assessment matrix, created in Excel, will be used to identify potential adverse events, their severity and likelihood of occurrence. The likelihood of occurrence can range from

unlikely to definite and the severity can range from significant to catastrophic. For risk assessments that yield borderline medium results, risk management strategies will be developed.

3.5.3 Ethical Compliance

Compliance with Health Insurance Portability and Accountability Act (HIPPA) laws is an important aspect of the project. Patient information must always be protected and if testing were to begin to involve patients, the team must take care to follow HIPPA laws. HIPPA certification will also need to be obtained in order for the team to view any surgeries first hand. This in-person experience with the surgery may help influence the design process by identifying the preferred surgical techniques in the operation room. Lastly, the team will make every effort to provide unbiased conclusions on testing outcomes.

4 ALTERNATIVE DESIGNS

4.1 Needs Analysis

The Needs Analysis process consists of a multi-faceted workflow. Beginning with the identified strategic focus, the process cycles through Needs Finding and Needs Screening, and then onto Concept Generation and Concept Screening. These four stages comprise the Identify and Invent phases of the Biodesign process (Biodesign, 2015). The Identify phase is detailed in this section and the Invent phase is outlined in section 4.2. The graphic outlining the phases is included below in Figure 11.

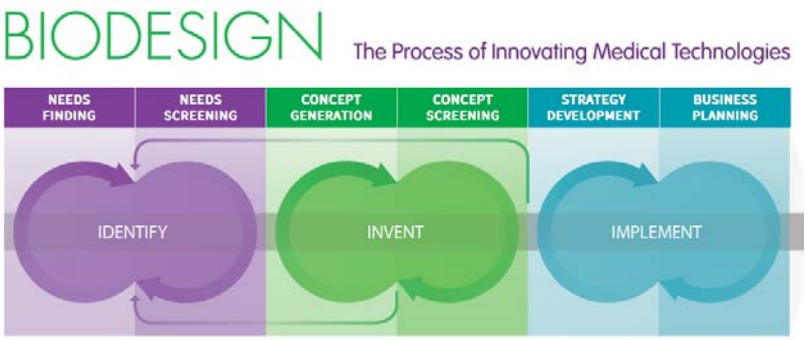

Figure 11. Three phase biodesign process workflow. (Biodesign, 2015)

4.1.1 Priority Needs

This project focuses on improving the outcome of rotator cuff repair surgeries for patients with large to massive sized tears. Based on the client statement, needs are divided into two sections: must-have and nice-to-have. The must-have needs are aligned with the project objectives and include the following bulleted list.

- Biocompatibility
- Adhesion of tendon to bone
- Device dimensions at least 3 centimeters long by 1 centimeter wide
- Adhere to FDA regulations

Biocompatibility: Critical to function of the design, biocompatibility ensures that the device can be implanted into a patient. This need is given a score of 10 on a scale from 0 to 10, with 10 being the most important. A biocompatible material needs to be used and tested during the

course of this project. Various compositions and coatings can alter PLA to be more biocompatible, and an on-campus object machine can print using a biocompatible material. The exact composition of this biocompatible material is proprietary and unknown at this time.

Adhesion of tendon to bone: Based on conversations with the project sponsor, Dr. Robert Meislin, the successful adhesion of the ruptured tendon to the bone enthesis is imperative. Adhesion of tendon to bone is rated a 10 on the equivalent scale. The device must not degrade over a period of 9 months, the typical timeline of the healing process. Further, the tendon-bone interface endures the greatest strain when the shoulder is abducted from -10° to 0° (Miyamoto *et al*., 2015). Finite element analysis (FEA) will be used to study where stress concentrations develop in the tendon using the new design, however some assumptions will need to be made. Most notably, FEA is most accurate when it does not reflect dynamic data. However, studies indicate that the greatest strain on the tendon occurs during dynamic abduction (Sano *et al*., 2007).

Device Dimensions: The target population for the device are patients with large to massive sized tears. These tears range from 3 centimeters to 5 centimeters, and greater than 5 centimeters in length. The average width of the tendon is approximately 21.9 millimeters (Sano *et al*., 2007). These dimensions will allow the team to construct physical models for testing and run FEA. The device must be geared to fit these dimensions and this need is given a score of 9 out of 10.

Adhere to FDA regulations: Following FDA regulations in the design of the device is inherent to the design process. The team will be sure to manage the restrictiveness of guidelines with the promise of new products for which there are not yet governing guidelines. This need is given a 7 out of 10 and is deemed a must-have because this need falls at the 50% threshold.

4.1.2 Non-Priority Needs

The following needs are categorized as nice-to-have.

- Use a bioadhesive to attach tendon to bone
- Use velcro-like design
- Not increase patient discomfort

- Arthroscopic delivery
- Potential application to other surgeries

Bioadhesive: A bioadhesive, like TCP - Tri Calcium Phosphate or poly-propylene fumarate might be used to help facilitate the attachment of the tendon to bone, as outlined in Section 2.8.1 and 2.8.2. This need is rated a 4 out of 10.

Velcro-like design: Although using a Velcro-like design was the initial prompt of this project, the client statement evolved to identify the core need, attaching tendon to bone, by any means possible. The Velcro-like design is not yet fabricated; however, the current standard is attachment by sutures which have a tensile strength of about 624 kilopascals (Jeon *et al*., 2015). The use of a Velcro-like design to hold the tendon to the bone would have to be at least as strong tensely as the sutures. This need is rated a 4 out of 10.

Maintain patient discomfort: Undergoing surgery of any kind is inevitably painful to some degree. Increasing patient discomfort by use of the design is unfavorable, however, it may be unavoidable. There are various pain scales available to physicians, such as the Numeric Rating Scale for Pain (NRS). This scale utilizes 11 points, ranging from no pain to “the worst pain imaginable” (Hawker *et al*., 2011). Ultimately, the design should aim to minimize the pain experienced by the patient, represented by a lower NRS score. This need is rated a 2 out of 10.

Arthroscopic delivery: Discussion with Dr. Meislin determined that developing the device for arthroscopic delivery is not within the scope of the project. However, he also said that it would be “nice-to-have.” The success of this objective can be determined by the sponsor successfully completing a trial surgery in a cadaver with the device. This need is rated a 2 out of 10.

Potential application to other surgeries: There is an opportunity for the device to be applied to repairs in similar surgeries, like meniscus repair. However, targeting these other surgeries is not within the scope of this project. This need is rated a 1 out of 10.

4.1.3 Technical Constraints

The largest technical constraint associated with the project is the limitations of testing methods. The *in vivo* conditions of the device will be modeled solely using in vitro techniques. As always, a discrepancy exists between *in vivo* and *in vitro* tests. Bovine tendons will be used to as the animal model for testing. The prototype devices will be appropriately sutured to the prepared tendon samples and will be pull tested on the Instron machine. The tendons are sized appropriately for the testing but are not identical models to the human supraspinatus *in vivo* or *in vitro.* Therefore, the tendon itself can have varying strengths based on its dimensions and the forces that the repaired tendon must withstand can also vary depending on the length and weight of the arm itself.

Further, in order to form conclusive data, a proper sample size must be tested. The industry norm for sample size is 30, however, for the purposes of the study, an n of 5 for each device and control was used.

4.2 Functions and Specifications

The primary function of the device is to be used during the surgical repair of large to massive rotator cuff tears. The device will function to reconnect the torn tendon to the bone in such a way that is comparable or superior to current state-of-the-art procedures. Further, the device will function to minimize retear failures due to mechanical failures of the tendon to bone adhesion. Ideally, the device must only begin to degrade after at least a nine-month period in order to provide enough mechanical support throughout the healing process. The device must be made from a proper biomaterial in order to be non-toxic to the human body as well as to minimize risk of infection. Secondary functions of this device are to promote healing once tendon to bone adhesion occurs and to encourage cell growth where the healed tissue will need blood supply and vascularization. In order to promote cell growth, the device must be osteoconductive such that it can provide a scaffold onto which bone-forming cells (osteoblasts) can come in and form deposition of healed bone. A final function is to eliminate the need for non-absorbable sutures that are an unfavorable treatment solution whereby they cause undue stress concentrations in the tendon. Overall, the clinical nature of this device works in order to decrease retear rates in patients undergoing rotator cuff surgeries for large to massive sized rotator cuff tears.

4.2.1 Concept Maps & Conceptual Designs

Based on the initial and revised client statements, each person in the group created a conceptual design drawing. Many more design alternatives were made based on established design functions and objectives in order to choose a final design that meets the client's needs. The main concepts that were involved in prototyping the designs were:

-Hook and loop, modeled after Velcro

-Press fit

-Suture-anchor augmentation, designed to thread sutures through the device itself

-One way prongs, barbs, or waves to oppose retractile forces of the tendon

-Using a bioadhesive to secure the device, or perhaps a bioadhesive on its own

Figure 12 outlines the concept map for the group's three most critical objectives for the project. Again, as these objectives relate to prototype design, the items listed under "Tendon to Bone Attachment" are applicable to the mechanical design of the prototypes.

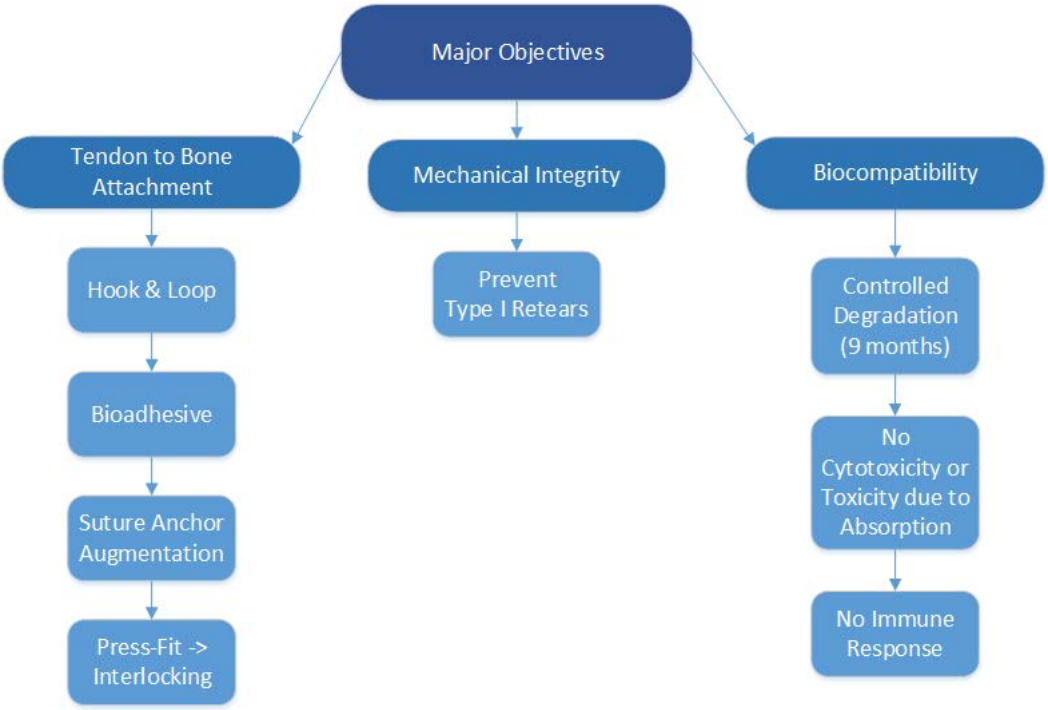

Figure 12: Concept map of the major objectives.

All preliminary final designs were developed as a group and iterated through based on trial-and-error testing.

4.2.2 Design Concept Prototyping & Modeling

The team worked to independently and cohesively design a variety of preliminary devices to allow for maximum depth of development. Designs include various features, such as interlocking geometric patterns, barbs, and potential incorporation of the current suture-anchor surgical methodology used in RCR surgery. The various designs are outlined in the following sections. Designs 4.2.2.1 through 4.2.2.5 are preliminary designs and Designs 4.2.2.6 and 4.2.2.7 are designs that are undergoing mechanical testing.

4.2.2.1 Barbed Tendon Interface 1

This design serves as an augmentation of the current suture-anchor surgical methodology employed in RCR surgery. As most Type I retears occur distally due to the sutures pulling through the tendon itself, effort was applied to improving the tendon interface rather than the bone interface. The premise of the design is to use multiple barbs that will pierce the tendon, increasing the surface area of tendon that the surgical fastener contacts and ultimately the friction between the tendon and the surgical fastener. Conceptually, increasing the surface area of contact makes sense to decrease the amount of stress on the critical components of the fastener (the suture in the case of a suture-anchor technique or the barbs on this fastener). The design will need to be verified such that its pull-out strength is greater or equal to that of the current gold standard, which for sutures, their tensile strength is roughly 624 kilopascals (Jeon *et al*., 2015). This will be tested at a later date *in vitro*. Two instances of the design will be used, one superior and one inferior to the tendon. The two fasteners will then be sutured together, where the suture will be passed through the superior fastener, the tendon, and then the inferior fastener, ultimately serving to provide a compression force. The barbs are oriented such that they will overlap when compressed, and will prevent the tendon from sliding in between the barbs. The distal ends of the surgical fasteners are barb-less, and will be sutured together and ultimately anchored with a surgical anchor into the humeral head. This part of the surgery will be carried out identically to the current suture-anchor methodology employed in RCR surgery. The design of one instance of the fastener can be viewed in Figure 13 below:

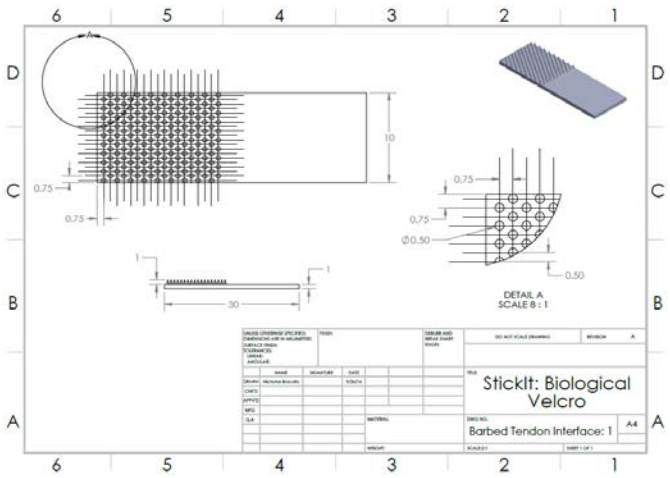

Figure 13. Drawing of Barbed Tendon Interface 1.

The device was then prototyped using the Qidi 3D printer, using PLA, an extruder temperature of 230 degrees Celsius, 30% infill, a layer height of 0.05 millimeters, a head speed of 60 millimeters per second when extruding and a head speed of 150 millimeters per second when traveling. The device was printed at a scale of 150%, and the result is shown in Figure 14:

Figure 14. Prototype of Barbed Tendon Interface 1.

The bottom portion of the model is composed of raft material, and would be removed in the final design. The left portion of the model should have resulted in barbs shown in the design drawing, however the result was a low-resolution pooling of material instead of functional barbs. The fastener is also noticeably rigid, indicating that the thickness of the material may be too great. Ultimately, the limitations of this method are as follows:

- The barbs, if printed correctly, are smooth and straight, and may pull out from the tendon graft. Moreover, other than a compression force from the suture, there is no retention method that prevents the tendon from ejecting from the fastener.

- The barbs are currently smaller than the Qidi printer's resolution of 0.1-0.2 millimeters. As a result, the morphology of the prototype was such that the molten PLA pooled where the barbs should have been printed. To counteract this, a revised barb design is necessary.
- There is no incorporation of a cellular scaffold at the current time, however after further investigations are conducted, adjustments to promote cell growth will be made. The device may block cell signaling and blood flow to the enthesis, impairing healing.

4.2.2.2 Barbed Tendon Interface 2

The second design is similar to the first, where barbs are the primary method for attaching the fastener to the tendon graft. In this case, the barbs are curved toward the distal end of the tendon graft and using a design analogous to barbed wire, incorporates a bar that prevents the barb from withdrawing. The bone interface is featureless, and like the first design, serves as an augmentation to the current suture-anchor methodology. Instead of using a suture to anchor the fastener, screw-like anchors are instead inserted through the fastener directly into the humeral head. In addition, unlike the first design, this design incorporates porosity, which aims to encourage cell migration and adequate blood flow such that biological healing can occur. The design is outlined in Figure 15:

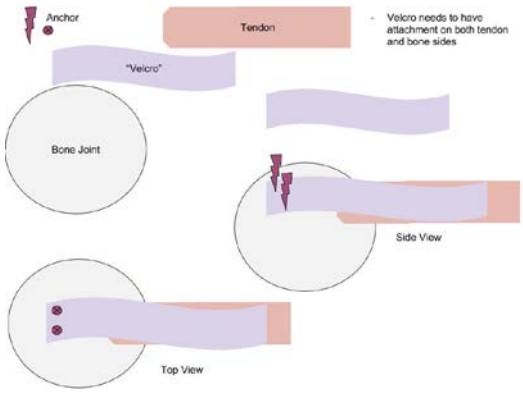

Figure 15. Schematic of Barbed Tendon Interface 2 (conceptual design).

This design has yet to be prototyped, however some limitations to this design are as follows:

- When printing the barbs, the Qidi 3D printer's resolution may be limiting, as some design features are less than the printer's resolution range of 0.1-0.2 millimeters. The size and shape of the barbs will need to be manipulated to facilitate the generation of an accurate prototype; moreover, the barbs will need to have dimensions greater than the minimum

resolution listed above, and as a result the barbs may not be able to pierce the tendon. This can be determined with simple *in vitro* tests involving a tendon sample.

- The porosity may not be great enough to facilitate adequate blood flow or cell migration. Testing of this property may be challenging. Also, given the restrictive resolution of the Qidi printer, accurately prototyping this feature will be challenging.

4.2.2.3 Hoop & Loop 1

This design concept utilizes two non-identical components. One component is a sheet with an array of hooks, and one component is a sheet with an array of looping structures, analogous to the design of commercially available Velcro. One sheet would attach to the tendon using a biological adhesive but due to limited adhesion in wet conditions and severe cytotoxicity, brought by fibrin glue an alternative of biological adhesive needs to be used such as a mussel protein-based bioadhesive (LAMBA) inspired by mussel adhesion and insect dityrosine crosslinking chemistry. LAMBA exhibited substantially stronger bulk wet tissue adhesion than commercially available fibrin glue and good biocompatibility in both *in vitro* and *in vivo* studies (Jeon *et al.*, 2015). The other sheet would attach to the bone in a similar fashion. The two halves would then connect in a fashion similar to Velcro, resulting in a fastened junction between the tendon graft and the humeral head. As an additive, polyurethane fumarate would be applied to the junction, serving as a facilitative medium to accelerate cell migration and ultimately the healing time. The preliminary design concept can be viewed in Figure 16:

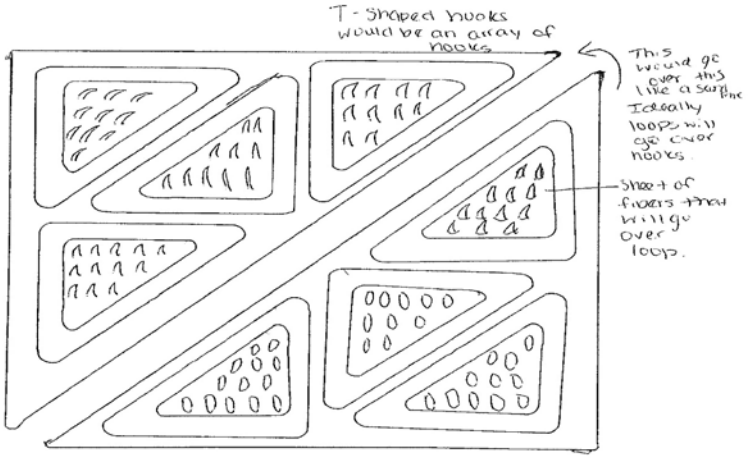

Figure 16. Schematic of Hook and Loop 1 (conceptual design).

This design was not prototyped. It was the basis for a conceptual design. There are some limitations that are immediately apparent:

- The looping structures will be difficult to prototype with the 3D printer, as there is an area of material that must remain vacant. To prevent failure of the looping structures during printing, a dissolvable support material may be necessary.
- The method for attaching the fastener to either the bone or the tendon interface remains mal defined. Biological adhesives propose an additional mechanical interface and thus another potential location for stress concentrations and ultimately failure of the tendon-bone junction. In such condition, finite element (FE) analysis will be useful to investigate stresses on implants and bones. Since soft tissue plays an important role in stabilizing a shoulder joint, load by muscle forces will greatly affect the result of analyses.
- The surgical methods necessary for implanting such a fastener differ vastly from the current standard, so adoption by surgeons may be difficult because of the potentially steep learning curve.

4.2.2.4 Square Insert

This design concept utilizes raised features with spaces in between for two instances of the fastener to adhere together. The tolerance is designed such that there is space between the features of the two halves of the fastener, so an interference fit is not utilized. Rather, an adhesive would be applied between the two halves, facilitating a strong attachment. The design incorporates various properties from design 1 and design 3, where like design 1, the assembly of the two halves of the fastener is created by simply duplicating one design instead of creating two different halves as in design 3. Like design 3, this design requires an adhesive or an alternative means to attach to both the tendon and the bone, and does not serve as an augmentation to the current surgical methods as designs 1 and 2 do. The preliminary design concept can be viewed in Figure 17a, and the assembly of two instances of the fastener can be viewed in Figure 17b.

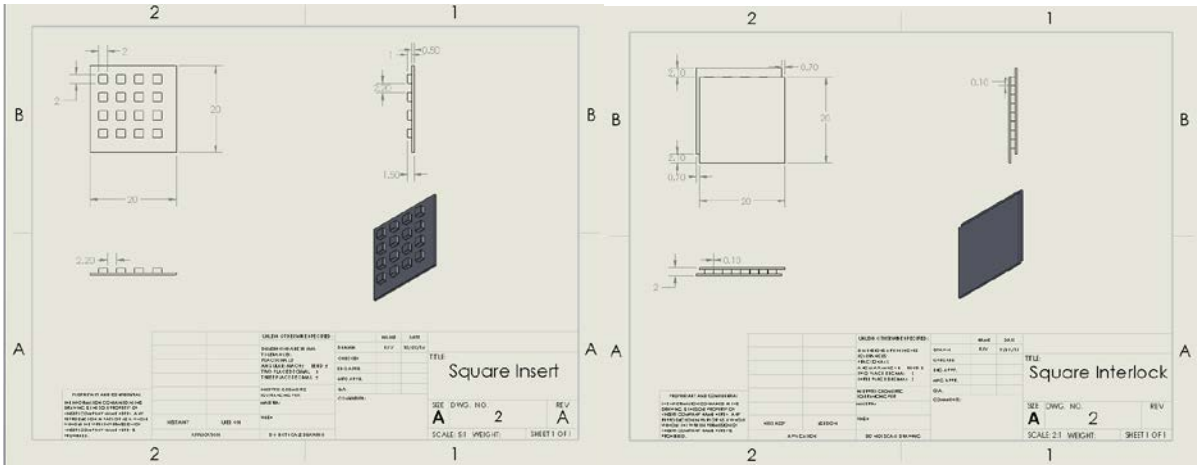

Figure 17. (A) Drawing of Square Insert (B) Assembly Drawing of Square Insert.

This design has been prototyped but not tested. Some limitations immediately apparent include:

- There is no compression force applied which would prevent the two halves of the fastener from separating. The attachment would potentially need to be facilitated by an interference fit or an additional adhesive after preliminary testing is completed. Specifically, the supraspinatus tendon is known to have the greatest stress between -10 to 0 degrees of abduction and therefore, the fastener would need to remain intact during these orientations (Parsons *et al*., 2002). The pullout strength of the fastener can be tested *in vitro,* and can be compared to the expected load at these orientations.
- The method adhering the fastener to the distal tendon being repaired and to the humeral head has yet to be determined. While the two halves of the fastener may form an adequate junction between themselves, the strength of the surgical repair may be limited by the methods incorporated for attaching the fastener to both the tendon and humeral head.
- Like design 3, the necessary surgical methods for implanting the fastener differ from the current suture-anchor method for RCR surgery. The fastener prototype is not flexible, and as a result cannot be passed through an arthroscope.

4.2.2.5 Clamp & Screw Design

The last final stage alternative design the team developed is a clamp-like design (Figure 18). The teeth in this design can grab onto the torn end of the tendon. Once the tendon is fully

inserted, a surgical screw can be drilled through the tendon to secure it into the clamp. The screw can either drill down into the bone, or the underside of the device can be secured to the bone using a bioadhesive. This device is 3D printed in MED610 and is not very flexible. The extended portion of material in the CAD drawing is for Instron testing purposes only.

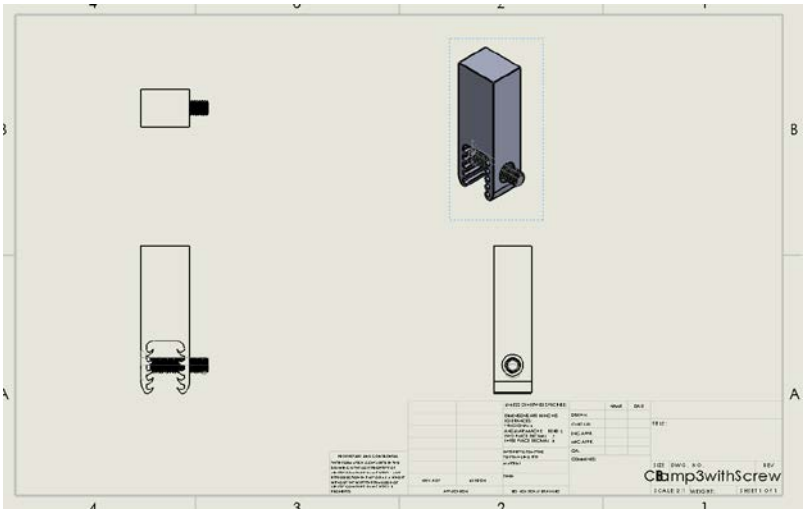

Figure 18. Clamp and Screw Device

4.2.2.6 One Way Barb Hinge Design with Suture Holes

This design has a removable hinge that allows the surgeon to easily maneuver it into place. The hinge should be placed proximally and removed after the device is sutured in place. One strip will rest on the top of the torn tendon, and the other will rest between the torn tendon and the bone. This device is an augmentation of the suture-anchor technique. The barbs are designed to oppose the force of the torn tendon as it tries to retract proximally to its torn state. Pairs of suture holes, dimensioned for the diameter of both the threading needle and suture, are placed along the length of the device to allow the surgeon to customize for the size of the tendon tear. The suture holes are also aligned so that when the hinge is folded around the tendon's thickness, the holes will line up. The entire design is 3D printed in MED610 and is flexible. The extended portion of material in the CAD drawing is for Instron testing purposes only (Figure 19).

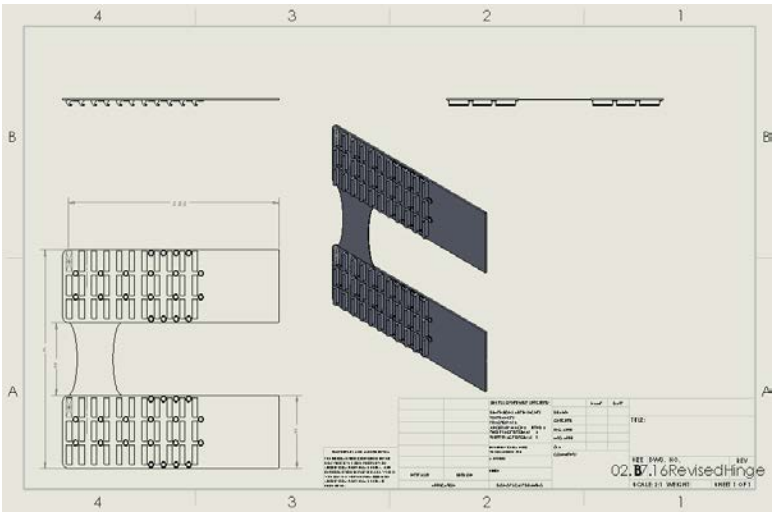

Figure 19. One Way Barb Hinge Design with Suture Holes.

4.2.2.7 One Way Barb, Diamond Interlock Design with Suture Holes

This design is placed between the tendon and the bone. First the surface of the bone is cleaned, and then thin component is placed along the bone such that the flat part is against the bone. A bioadhesive is used to secure the flat surface to the bone. The thicker component is secured to the underside of the torn tendon using a bioadhesive, or sutures if necessary. The one-way barbs should be oriented so as to oppose the force of the torn tendon as it tries to retract to its torn state. This direction will point distally from the patient's centerline. Then, the diamond interlock interfaces can be press fit together at the desired distance. If necessary, I thin layer of bioadhesive can be applied to the diamond interlock interfaces to further reinforce the tendon to bone attachment (Figure 20). This design is not used in conjunction with suture anchors. Finally, the design is 3D printed in MED610 and is flexible to a degree that has yet to be quantified. The extended portion of material in the CAD drawing is for Instron testing purposes only.

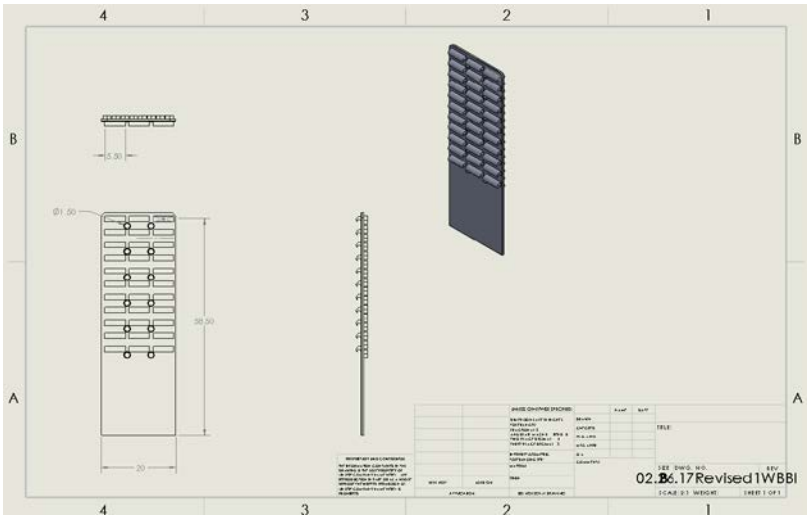

Figure 20. One Way Barb Hinge Design with Suture Holes.

4.2.2.8 Design Selection

The team will conduct mechanical testing on the two final designs. From the data gathered, it will determine which design is the best to move forward with as the official prototype. All preliminary final designs have been iterated multiple times to ensure the team's confidence in their suitability for testing. Additionally, all mechanical testing will be conducted using bovine tendons, sutures, and the Instron 5544 machine. A BlueHill method was developed and will be used across all samples. Once the data files were obtained, a MATLAB code was developed to analyze the data and statistical analysis was performed on the resulting values. Statistical analysis tests included ANOVA and t-tests assuming equal variances with an alpha level of 0.05.

4.2.3 Feasibility Study

Once all preliminary designs were established, proof of concept needed to be tested in order to evaluate the designs. It was important to conduct this analysis before committing to one design in efforts to be conscious of time and resources. Specifications such as biocompatibility and mechanical integrity were analyzed in addition to resolution and precision size of the designs printed by the machine. A reach goal is to analyze the fatigue the devices are able to withstand through cyclic testing as well as to perform flexure testing to quantify the devices' flexibility.

4.2.3.1 Biocompatibility

The end design of this project will be implemented into the body and therefore, it is imperative that the device does not release any cytotoxins and only causes minimal patient discomfort. Two elution assays were conducted using a double sterilization technique on each of the test materials. It was also imperative that all supporting materials, stir bars, forceps, and media bottles, were also sterilized so that there was no contamination. Specifically, 4, 100 milliliter media bottles, 6, 1 centimeter magnetic stir bars and 4 pairs of stainless steel forceps were sterilized via autoclaving.

The concentration of test material to media chosen was 50 micrograms/milliliter, and this was based on how much material could be realistically submerged. To accomplish this, each material was cut into approximately 3 centimeters long segments and massed such that there was 8 grams total of the material per 160 milliliters of complete media. The PLA or MED610 was then sterilized by first submerging each material in 70% isopropyl alcohol for 3 hours and then subjecting it to UV light for 30 minutes. To do this, the strips of PLA or MED610 were removed from the isopropyl alcohol using sterile forceps and placed on petri dishes such that the strips were not overlapping. The dishes were then incubated in a UV chamber for 30 minutes, removed, and 4 grams of test material was inserted into each of two sterile, 100 milliliter media bottles. 160 milliliters of complete media were prepared with 88% Dulbecco's Modification of Eagle's Medium (DMEM), (Cellgro Catalog # 15-013- CV, with four and half grams per liter glucose and sodium pyruvate without L-Glutamine), 10% Fetal Bovine Serum (FBS, Atlanta Biologics, Catalog #S11150), 1X Glutamax (GIBCO, Catalog # 35050-061), and 1% Penicillin/streptomycin (Lonza, Catalog # 17-603). The components were added to each of the media bottles via a transfer pipette. One stir bar was placed in each media bottle using different sterile forceps, the bottles were sealed, and they were stirred using a wireless magnetic stir plate set to max for one week in a 4°C refrigerator.

Approximately 100,000 NIH-3T3 cells were plated in each well of a 6 well plate using complete medium supplemented with 10% FBS, 1% Penicillin/streptomycin, and 1X Glutamax. The cells were incubated for 48 hours checked to determine confluency. If the cells reached 80% confluency, media could be changed to the media supplemented with the respective materials (experimental media). 3 milliliters of the experimental media was added to each well and incubated for 24 hours. After this 24-hour incubation period, the wells were stained and counted

according to Tables 4-6. Three well plates were prepared: one control plate in which the media was exchanged for media not supplemented with the materials, and two plates in which the media was exchanged for media that was supplemented with MED610 or PLA.

Table 4: Well Designation for Control Media Study

Plate 1	Control -> Stain (+)	Control -> Stain	Control -> Stain
	Control -> Cell Count	Control -> Cell Count	Control -> Cell Count

Table 5: Well Designation for PLA Media Study

Plate 2	PLA-> Stain (+)	PLA -> Stain	PLA -> Stain
	PLA -> Cell Count	PLA -> Cell Count	PLA -> Cell Count

Table 6: Well Designation for MED610 Media Study

Plate 3	MED610 -> Stain (+)	MED610 -> Stain	MED610 -> Stain
	MED610-> Cell Count	MED610-> Cell Count	MED610-> Cell Count

Twenty milliliters of DPBS (with Calcium and Magnesium) was prepared with Hoechst 33342 and Propidium Iodide stains at concentrations of 0.5 micrograms/mL and 0.2 micrograms/mL, respectively. The Hoechst stain was used to visualize all cells, live or dead, and the Propidium Iodide was used to visualize any dead cells in the wells. Wells 1, 2 and 3 of the 6 well plate were aspirated, rinsed 3 times with DPBS (+), only aspirating well 1 after the third rinse. At this point, 3mL of ice cold methanol was added carefully to well 1, allowing the plate to stand for 10 minutes such that the cells would be fixed. The fixative was aspirated, the well was rinsed twice, and wells 1-3 were then aspirated and 3 mL of the stain-containing DPBS (+) was added to each well. The plate was incubated without exposure to light for 15 minutes, the stain was aspirated and 3mL of DPBS (+) was added to each well.

The first 3 wells were imaged using a fluorescent microscope, using a DAPI filter to visualize the blue Hoechst stain, and a rhodamine filter to visualize the red Propidium Iodide stain. For each well, a phase contrast image was taken with an exposure time of 500ms. Then, The Hoechst and Propidium Iodide stains were visualized using their respective filters, at an exposure time of 500ms for the DAPI filter and 2000ms for the rhodamine filter. The stains were taken using a two channel setting on the scope, allowing the two stains to be overlaid in one field of view. After the image was taken, the background noise was removed and the gain was adjusted for each filter, making the images sharper. Once all the images were captured, the presence of cells staining positive for propidium iodide were compared well to well. If a well contained a significant amount of red cells, the cells were identified as dead, and conclusions regarding the cytotoxicity of the media or additives to the media could be made.

Concurrently with the staining process, the cells in wells 4, 5, and 6 were trypsinized and combined into one 15 mL conical tube. The cells were suspended in 10 mL complete medium, and then three 10 microliter sample were taken of the suspension, transferred to three hemocytometers, and then counted. This was conducted on the three well plates: the two plates in which the media was exchanged for material-supplemented media at 48hours, and the control plate where unsupplemented media was utilized. The cell numbers were compared amongst the three experimental groups: a hypothesis test for mean was conducted to determine if the cell numbers of the two material-supplemented media groups were significantly less than that of the control group. An alpha value of 0.05 was used.

4.2.3.2 Resolution Capabilities

After drafting designs in CAD, functionality tests for the Qidi printer were conducted to determine its precision and resolution. It is important to analyze any printing device for this project in order to gain a deeper understanding of how the team can use or manipulate its settings. The final device design was highly dependent on how specific the printer can create the necessary details for making tendon adhesion possible. The group found that the Qidi printer did not have a high enough resolution. Therefore, the team pivoted to use the Object Connex 360 printer to create the prototypes. The Objet machine can print using MED610, a biocompatible material, and does so at the resolution required of for the project. The trade off when using the Objet printer is that there is a longer lead time in obtaining prints, it is more expensive, and the

cleaning method can damage the part. Part cleaning is performed by pressure washing the printed support material off of the surface of the device. Unfortunately, some of the more delicate or flexible features of the prototypes may be damaged when the cleaning is performed.

4.2.3.3 Mechanical Property Testing

Baseline tests for mechanical properties of PLA and MED610 were completed in order to understand properties of the materials before final selection of the printing material. They followed the ASTM D638 testing protocol. Samples were appropriately dimensioned into a small dog bone shape and 3D printed in PLA (n=2) and MED610 (n=3). All samples were loaded onto the Instron using the top and bottom grip and were pulled to failure in the Instron 5544 using a 2000 N load cell and 20 mm/min extension rate. A BlueHill Software 3.2 method was created and data collection was processed using MATLAB. Tensile testing was first conducted on the samples using the Instron 5544. The equations below were used to assist in the calculations of the mechanical properties obtained stress strain curve. These properties include the maximum force, young's modulus, and ultimate tensile strength (UTS).

Engineering Stress: $$\sigma = \frac{F}{A} \quad (1)$$

Engineering Strain: $$\varepsilon = \frac{l_f - l_i}{l_i} \quad (2)$$

Young's Modulus: $$E = \frac{\sigma}{\varepsilon} \quad (3)$$

The maximum force is an output directly from the developed Bluehill method. Based on the 2000N load cell used, a continuous force vs. displacement curve was obtained for each sample. Each sample was dimensioned using a caliper prior to testing, and the cross sectional area for the sample was used to calculate the stress values using Equation 1, implemented in the MATLAB script. Extension rate and gauge length measurements are used to calculate the strain values throughout the test. The MATLAB script uses a moving window function to calculate the instantaneous Young's Modulus at each point along the newly developed stress vs. strain curve. From these values, the function isolates the curve after the toe region and before the yield point. This linear portion of the stress vs. strain curve gives the Young's Modulus of the material.

Finally, the ultimate tensile strength (UTS), was calculated by dividing the maximum force by the original area to understand the maximum stress before fracture. All data collected and analyzed during these initial experiments was conducted using Bluehill Software in conjunction with MATLAB.

4.2.3.4 Tendon Suture Pull-Through Testing

Suture pull-through testing was conceived as the control model to represent the mechanical properties of a Type I retear. The control testing was first conducted with an inaccurate suturing stitch that is not representative of surgery standards. Therefore, this data gathered for control purposes became irrelevant. Subsequently, the control was re-stitched using the Mason Allen stitch. This test has a sample size goal of n = 5. All parameters outlined in Section 4.2.3.3. Mechanical Property testing, similarly apply to pull-through testing. These parameters include Young's Modulus, maximum force, and UTS. The averages for these parameters across the control samples will be used in comparison to experimental conditions that model how the prototyped devices would help mitigate Type I retears.

In order to prepare bovine tendons for testing, frozen bovine specimens were thawed in saline solution for one hour. Once thawed, the outer sheath was removed to reveal the tendon. The tendons were cut down to have a cross sectional area of about 6 mm by 2.5 m. For all sample groups involving sutures a #2 suture (Anthrex #2 FiberWire Suture w/ Tapered Needle, CN: AR- 7200) was used. For suture pull-through tendon control a modified Mason Allen stitch was used to closely model the current surgical technique. For the control testing the samples were loaded onto the Instron as follows: the top end of the tendon was attached to the top grip while the bottom stitch was attached to the bottom grip of the instron.

4.2.3.5 *In Vitro* Simulation

The standard operating procedure for the *in vitro* testing can be found in Appendix A.3.

5 DESIGN VERIFICATION

5.1 Client Feedback

Throughout the design process multiple design feedback meetings were held with Dr. Meislin. During these meetings, the group presented available prototypes and talked through prioritizing designs. This feedback was important to the design process because it helped ensure the final design was feasible and usable for the user. Transcripts of the meetings can be found in Appendix B.

5.2 Testing Results

5.2.1 Biocompatibility Results

The biocompatibility of the materials was tested using the procedure outlined in Appendix A.2. All of the notebook documentation can be found in Appendix D. The final results were drawn from two different experimental groups: one 6-well plate with approximately 100,000 NIH/3T3 cells (per well) seeded on 31 January 2017 and a duplicate plate seeded on 3 February 2017. The first well plate was used to test the biocompatibility of MED610 and the second was used for testing with PLA. Imaging was performed using the Zeiss Zen software suite, utilizing a 500ms exposure time for imaging with the DAPI filter, and a 2000ms exposure time for the rhodamine filter. An exposure time of 500ms was also utilized for phase contrast imaging.

The imaging results are as follows in Figure 21. All wells were imaged with approximately 80% confluence, as indicated by the approximate density of blue-fluorescing cells in the Hoechst-stained images as well as the phase contrast images of all experimental replicates. The methanol-fixed cells elicited 100 percent cell death, as indicated by the red fluorescence from the propidium iodide stain. The negative control wells, in which no media-soaked media was utilized, elicited no apparent cell death, as indicated by the lack of red fluorescence from the propidium iodide.

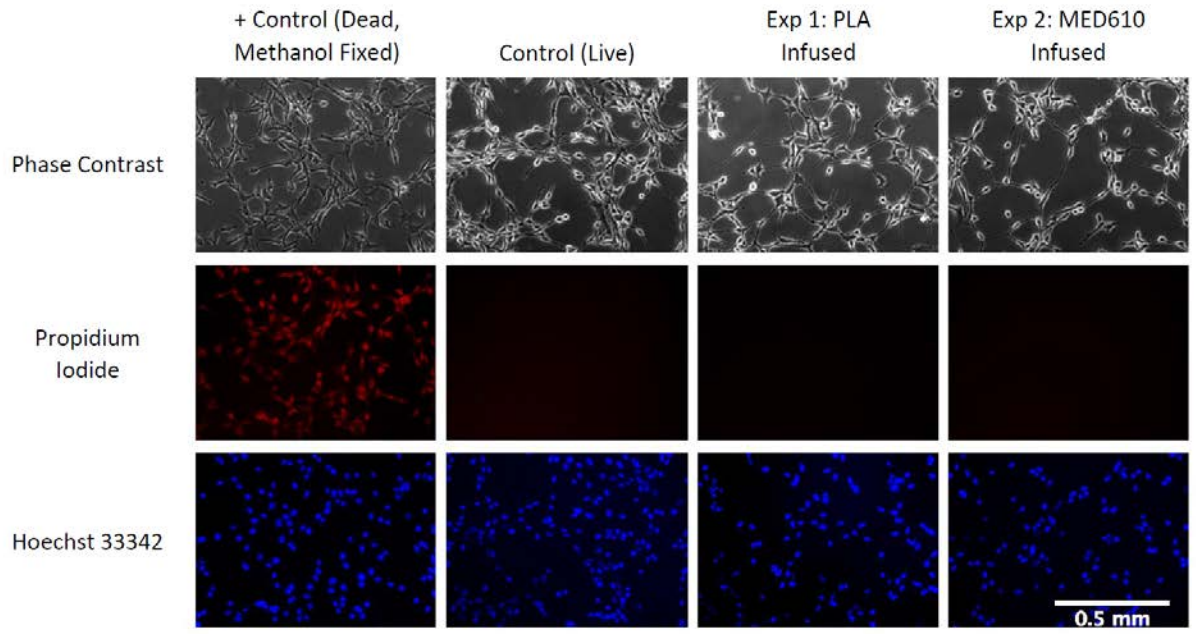

Figure 21: Phase contrast (row 1) and fluorescence images (rows 2 and 3) in the control and experimental groups.

The cell counts for each replicate are displayed in Table 7 which displays the pooled cell numbers for the control, PLA, and MED610 experimental conditions. Also displayed are the p-values for the hypothesis test stating that the cell counts of the material-infused conditions are identical to that of the control as the null hypothesis. For each duplicate plate, the cell populations from 3 wells were pooled and 3 separate cell counts were performed on the pooled samples. The results for each experimental condition are outlined in sections 5.2.1.1 and 5.2.1.2.

Table 7: Cell Counts for NIH/3T3 Cells Plates

Trial (#)	**Control Media [10^6 cells]**	**Media with PLA [10^6 cells]**	**Media with MED610 [10^6 cells]**
1	2.25	2.43	2.34
2	2.79	2.79	2.34
3	2.16	2.43	1.98
AVERAGE	2.40	2.55	2.22
SD	0.34	0.21	0.21
P(T<=T)	N/A	0.55	0.48

5.2.2 Resolution Capabilities

At the beginning of the project, prototypes were printed in PLA by the Qidi printer. The team assembled, took online training, and performed troubleshooting the Qidi printer in a number of ways. One issue with the printer was that the prints would be engraved and melted into the build plate. In order to prevent this from happening, Kapton tape was applied to the build plate to allow the finished prints to be easily removed. Files were printed by first developing the prototypes in SolidWORKS, exporting to a .stl file, and converting the .stl file into an .x3g file using the Qidi printer software. Extrusion rates were approximately 260 mm/second and the extruders were maintained at 212 ^{0}F throughout pr calibrated and all prints were closely monitored to prevent a myriad of errors from occurring. Resolution of the prints was low and the Qidi printer was unable to produce high quality prints.

WPI's Rapid Prototyping Lab has a number of 3D printers available to the school. One of these printers is the Objet Connex260 that is capable of printing in MED610. As previously described, MED610 is a proprietary biocompatible material. The prints were created using a cartridge for both printing and support material. The support material must be removed from the print by power washing with water. Print resolution for these parts is very detailed and allows small features of the prototypes to translate from the CAD model to the physical print.

After visually inspecting the Qidi printed PLA prototypes compared to the Objet printed samples, a difference in resolution was apparent. The Qidi printer was simply not exact enough when printing finer features for the project applications. Therefore, all preliminary final prototypes were manufactured using the Objet260 Connex printer.

5.2.3 Mechanical Properties of Materials

Mechanical property testing is outlined in section 4.2.3.3 and section 4.2.3.4. All recorded data can be seen in the following tables for the Bovine Tendon Control (Table 8), PLA (Table 9) and MED610 (Table 10).

Table 8: Bovine Tendon Control Parameter Values

Bovine Tendon: Control			
Sample	Max Force (N)	Max Stress (MPa)	Young's Modulus (MPa)
Sample 1	508.5182	6.8275	0.9042
Sample 2	795.9860	8.1740	1.0671
Sample 3	509.3809	8.0633	0.5278
Sample 4	332.8959	3.8035	0.1551
Sample 5	858.8883	16.3145	3.0547
Mean	**601.1339**	**8.6366**	**1.1418**
St. Dev.	**191.7515**	**2.0360**	**0.2766**

All values for the control parameters are within the upper and lower fences as defined by calculating the interquartile ranges and final n = 5.

Table 9: PLA Parameter Values

PLA			
Sample	Max Force (N)	Max Stress (MPa)	Young's Modulus (MPa)
Sample 1	542.6000	4.9900	41.6200
Sample 2	397.1700	3.8100	36.7600
Mean	**469.8850**	**4.4000**	**39.1900**
St. Dev.	**102.8345**	**0.8344**	**3.4365**

All values for the PLA parameters are within the upper and lower fences as defined by calculating the interquartile ranges and the final n = 2.

Table 10: MED610 Parameter Values

MED610			
Sample	Max Force (N)	Max Stress (MPa)	Young's Modulus (MPa)
Sample 1	802.5900	7.6700	59.2900
Sample 2	893.5800	7.1300	79.2000
Sample 3	942.8700	7.8900	80.6400
Mean	**879.6800**	**7.5633**	**73.0433**
St. Dev.	**71.1655**	**0.3911**	**11.9325**

All values for the MED610 parameters are within the upper and lower fences as defined by calculating the interquartile ranges and final n = 3.

5.2.4 *In Vitro* Simulation

In vitro stimulation is outlined in in Appendix A.3, recorded data can be seen below in tables for Bovine Tendon Mason-Allen Suture Control (Table 11), Hinge-Wave Design (Table 12) and Diamond Interlock Design (Table 13). All sample groups have an n = 5.

Table 11: Bovine Tendon Suture Pullthrough Control Parameter Values

Bovine Tendon Suture Pullthrough: Control			
Sample	Max Force (N)	Max Stress (MPa)	Young's Modulus (MPa)
Sample 1	91.1125	15.3130	28.9110
Sample 2	259.5087	31.0400	114.1750
Sample 3	164.1353	26.3670	128.9660
Sample 4	177.7070	28.5470	155.6700
Sample 5	196.3239	25.5290	37.1110
Mean	**177.7575**	**25.3592**	**92.9666**
St. Dev.	**54.2603**	**6.0084**	**56.7900**

All values for the control parameters are within the upper and lower fences as defined by calculating the interquartile ranges.

Table 12: Hinge Parameter Values

Hinge: Experimental			
Sample	Max Force (N)	Max Stress (MPa)	Young's Modulus (MPa)
Sample 1	418.9300	14.6400	53.8500
Sample 2	349.5500	12.4300	15.1900
Sample 3	398.3300	13.4700	71.6800
Sample 4	344.6700	11.6100	65.8700
Sample 5	297.1600	11.4100	63.7700
Mean	**361.7280**	**12.7120**	**54.0720**
St. Dev.	**48.0106**	**1.3492**	**22.6669**

All values for the Hinge experimental parameters are within the upper and lower fences as defined by calculating the interquartile ranges.

Table 13: Interlock Parameter Values

Interlock: Experimental			
Sample	Max Force (N)	Max Stress (MPa)	Young's Modulus (MPa)
Sample 1	105.9554	4.0000	37.3140
Sample 2	134.3434	5.1300	26.6450
Sample 3	135.0701	6.2800	45.9190
Sample 4	95.2095	4.3300	5.3690
Sample 5	208.1169	9.5600	64.3250
Mean	**135.7391**	**5.8600**	**35.9144**
St. Dev.	**39.4225**	**2.2472**	**21.9554**

All values for the Interlock experimental parameters are within the upper and lower fences as defined by calculating the interquartile ranges.

6 DISCUSSION

6.1 Final Design Evaluation

After conducting a series of mechanical testing as described in the previous chapter, it was determined that the most beneficial design to fit the needs of the patient and surgeon was the Hinge-Wave design. Throughout the design process, the group was in constant contact with Dr. Meislin for feedback on all designs and initially, before *in vitro* testing, his favorite design was the Diamond-Interlock prototype. The major part of this design that needs improvement is how the device will be delivered due to size and manipulation of the material. Now that this prototype has shown potential, new materials would need to be tested in order to make it more flexible for delivery. However, the ease of reproducibility of this design outweighs that issue. Dr. Meislin was also very fond of the mechanical properties of this Hinge design as they showed to be more promising than other designs or the current surgical protocol.

6.2 Economics

This final product of this project will potentially enter the medical device market, which has been projected to reach a market size of $155 billion by the close of the 2017 fiscal year (Medical technology spotlight: Select USA.2017). The medical device industry has a broad spectrum of products ranging from single use tongue depressors to multiuse magnetic resonance imaging (MRI) machines. With an addition to the market, such as a surgical fastener for rotator cuff repairs, it would have to be competitive to produce revenue, but affordable to allow for surgeons to use this product compared to the current suture and suture anchor options. The fastener should not take any longer to insert as compared to the current surgical techniques in order to keep operating room costs low and practical for surgical application usage. Finally, the mass production of this device must be done at a low experience rate to allow for a greater return on investment in addition to influencing surgeons to favor this device. FDA compliance will need to be ensured, along with successful performance in clinical trials before the device could enter the medical device market.

6.3 Environmental Impact

With the surgical fastener, the two largest negative environmental impacts would be due to the manufacturing and packaging processes. In a study conducted at UC Berkeley, the Objet

PolyJet technology was compared to a computer-controlled mill (CCM) against “materials and manufacturing of the machines themselves, transportation, energy use, material in the final parts, material wasted, and the end-of-life disposal of the machines, (Faludi, 2013).” Unfortunately, the Objet printer wastes about 40% of its material cartridge which is more of a sustainable problem than an environmental one. However, if this manufacturing method is conducted for approximately 6 hours a day, 5 days a week, the Objet printer is “roughly ten times the impact of the same (CCM) machine at maximum utilization (Faludi, 2013).” An alternative manufacturing method should be sought if environmental impact is to be decreased. Alternatively, Object would need to revise their printer such that it optimized for minimal material loss.

As far as packaging is concerned, currently, every company aims to reduce emissions and expenses associated with packaging. By implementing packaging materials and processes that are latex, PVC, and mercury-free, as well as free from any bio-accumulative toxins, the device will then have a greater positive impact on the marketplace. Many of these initiatives are associated with Six Sigma, which is an operational excellence methodology used in various industries to better an organization and increase customer satisfaction (Six Sigma, 2017). With this in mind, it is crucial that this surgical fastener abide to these environmental restrictions and a new manufacturing process be identified once a final material is chosen and final specifications are outlined.

6.4 Societal Influence

When advancements or changes in technology occur in society, they have the potential to be both beneficial and also harmful. This device may not only impact the patient or surgeon but also the general population. For example, with this new device, job opportunities in a variety of departments may develop; however, other jobs relating to the gold standard approach may be jeopardized. The greater efficiency the device has compared to the current options, the more plausible it will become the preferred method for surgery. Likewise, with rehabilitation, a shortened recovery period would aid patients, but may affect the physical therapy business associated with post-surgery treatment. Moreover, the number of hours billed for by physical therapists would decrease, thus decreasing their income.

6.5 Political Ramifications

With any novel device, there could be potential for political ramifications. Specific to the medical device industry, under the Affordable Care Act, all manufacturing companies must pay a 2.3% sales tax on any device-related revenue. Although many large-name companies may not worry about a small percentage, this law directly affects the small to medium sized start-up companies, which together compose of 80% of medical device company market (Medical technology spotlight: Select USA.2017). Although this surgical fastener could drastically alter surgeries, it may be difficult to upscale manufacturing and productivity if this taxation greatly affects the financial statements. Moreover, the growth of the small start-up operations may be hindered due to the restrictions that are imposed by the 2.3% sales tax.

6.6 Ethical Concern

This surgical fastener is considered to be a Class III medical device, which means it will be implanted directly into the patient for an extended amount of time. With this being said, testing of this device and its prior prototypes would need to be completed in an *in vivo* setting. During this testing, it is imperative that the protocols are conducted properly in order to ensure safety of all animal models. In clinical trials, it would be imperative that patient consent is explicit, and they are fully aware of the risk associated with participating in such a trial

6.7 Health and Safety Issue

As a Class III implantable device, it is imperative that the user and patient safety are thoroughly considered. The device must not leach toxins, stimulate an allergic response, or cause bacterial or viral infections. Additionally, it is important to understand how the device will react in the body over a shorter and longer period time in order to alter any design components.

The device will need to be surgically sterile and manufactured in a quality controlled cleanroom. Given the particulate size constraints, the cleanroom would need to be at least a Class 8 level cleanroom. The devices will be sterilized using ethylene oxide gas (EtO). This method of sterilization exposes the product to ethylene oxide in a large, closed, sterilization machine. EtO works by permeating the membrane of any microbes present and destroying the nucleic components of the pathogens through strong alkylation reactions (Mendes *et al*., 2007). Prior to EtO exposure, the product along with a biological indicator (BI) will be sealed inside an

appropriate bag and EtO tape will be placed on the outside of the bag. After EtO exposure, the tape will appear striped - indicating to customers that the product has been properly sterilized. Further, by including a BI within the container, surgeons can double check each product for sterilization before even opening the bag.

6.8 Manufacturability

For the final design of the surgical fastener, it would be strategic to use mass production manufacturing methods to decrease the cost of developing one unit as well as making the device more available. The manufacturing process would comply with current good manufacturing processes (cGMP) and be ISO9001 certified, meaning that a proper Quality Management System (QMS), is in place. A tracking system will be utilized to track all products in order to perform root cause analysis, should any corrective and preventative action (CAPA) need to be taken.

At this time in the project, evaluation of an optimal material and 3D printer is unknown due to limitations of testing availability and budgeting. With these constraints identified, it was then recommended to use the current approach with the Objet 3D printer filled with MED610 cartridges along with SUP705 fill material. If this device concept is then purchased by a large company or a significant amount of grant money is obtained, multiple Objet printers will be utilized in a Class 8 level cleanroom to produce the devices at a quick rate. Typically, one device can be printed and cleaned within 10 minutes, which results in a production of approximately 40 per day. Based on the pricing of the MED610 cartridge, each device costs about $15 to manufacture based on a $9 cost for materials and additional costs for labor. Finally, the cartridge holds enough material to print approximately 200 parts, allowing for a high production throughput.

6.9 Sustainability

By using 3D printing manufacturing methods, there is potential for environmental risks. However, once the product is adopted as a viable solution for rotator cuff repair and becomes commonly used in various surgical applications, the manufacturing company could focus their efforts toward ensuring greener outlooks at the manufacturing plant in order to reduce emissions, reduce waste fill material and/or other products. By continuously improving manufacturing and

developmental methods to cohesively work with sustaining efforts, this medical device would prove itself successful from both an efficacy and sustainability perspective.

7 FINAL DESIGN & VALIDATION

Through both biocompatibility, mechanical property analysis, and statistical analysis of the in vitro testing, the final Hinge device has proven to be successful. These three tests ensure that the final overall design met each of the objective formed at the beginning of the project. By conducting each of these tests, the team was able to determine it would be simple and efficient to create this fastener to be used in conjunction with sutures in order to infiltrate the current market. Although great strides have been made throughout this design process, many tests and studies need to be further conducted in order to surpass all FDA requirements for implanted medical devices.

7.1 Result Analysis

The following sections outline the testing results for biocompatibility testing and mechanical testing. Mechanical testing is comprised of two parts: material property testing and *in vitro* device testing.

7.1.1 Biocompatibility

Soaking PLA in complete media for one week and then incubating cells for 24 hours with the media did not elicit a cytotoxic response, as concluded by the lack of dead cells. In Figure 21 (section 5.2.1) when observing the results in column 3, there are no red-fluorescing cells in row 2, and all of the cells fluoresce blue in row 3, showing that 100% of the cells plated in the PLA-infused media are live. When comparing the cell population numbers of the PLA-infused media against the control state, there is no significant difference ($p=0.55$), and therefore it can be concluded that cell proliferation was not affected by the altered media.

From the same protocol, the soaked MED610 in complete media for one week was then incubated with cells for 24 hours and the media did not elicit a cytotoxic response, as concluded by the lack of dead cells. In Figure 21 when observing the results in column 4, there are no red-fluorescing cells in row 2, and all of the cells fluoresce blue in row 3, showing that 100% of the cells plated in the MED610-infused media are live. When comparing the cell population numbers of the MED610-infused media against the control state, there is no significant difference ($p=0.48$), and therefore it can be concluded that cell proliferation was not affected by the altered media.

Overall, there was no red fluorescence present in the experimental groups, indicating no cell death. MED610 and PLA did not elicit a cytotoxic response. There was no significant difference in the cell number of the MED610 condition compared to that of the control condition ($p = 0.48$) as well as no significant difference in the cell number of the PLA condition compared to that of the control ($p = 0.55$). Thus MED610 was chosen as the final material selection due to the resolution of the Object printer.

7.1.2 Resolution Capabilities

The Objet printer has more favorable resolution and throughput than the Qidi printer. Therefore, all tested prototypes for *in vitro* simulation were prototyped in MED610 using the Objet printer.

7.1.3 Statistical Analysis of Material Mechanical Properties

A one way ANOVA test, pictured in Table 14, shows that there are no significant differences among the parameters for the three material property test groups. For both the max force and max stress parameters, there is no significant difference between the two material options and the control. In the Young's Modulus data, there is statistical significance between the groups. However, this significance was disregarded because the failure mode of the tendon is more prolonged than that for the material samples. As the tendon is failing, it first reaches its maximum force and stress, and then the force and stress values plumm*et al*most to zero. The tendon fibers begin to fray and one by one they give way, all while the force values and subsequent stress values, remain plateau-d. This region of the curve indicates that the Young's Moduli values are not comparable across sample groups. Therefore, the significance between the sample groups regarding only Young's Modulus is disregarded. Table 14 below shows the areas of significance between the sample groups based on ANOVA testing performed in Excel.

Table 14: ANOVA Based Significance for Material Choice

ANOVA Material Choice			
Parameter	F value	F critical value	Significance
Max Force	3.8321	4.737414	No
Max Stress	1.031609	4.737414	No
Young's Modulus	114.7529	4.737414	Yes

Overall, MED610 and PLA were evaluated based on biocompatibility, mechanical properties, and print resolution. No significant difference was found between the two materials regarding biocompatibility and mechanical properties. Therefore, the MED610 material was selected for prototyping because it produced a favorable 3D printing resolution.

7.1.4 Statistical Analysis of *In Vitro* Simulation

A one way ANOVA test shows there are significant differences between the maximum force and maximum stress parameters across the three samples: Hinge, Interlock, and Control. There is no significant difference between the three sample groups for Young's Modulus. Table 15 below shows the F values and F critical values for the ANOVA tests on each parameter. ANOVA tests shows significance among the sample groups when the F value is larger than the F critical value. When the F value is less than the F critical value, there is no statistical significance among the data pool.

Table 15: ANOVA Based Significance for In Vitro Simulation

ANOVA In Vitro Simulation			
Parameter	F value	F critical value	Significance
Max Force	27.3397	3.8853	Yes
Max Stress	34.1578	3.8853	Yes
Young's Modulus	3.0191	3.8853	No

After significance was found in the maximum force and maximum stress parameter groups, further statistical t-testing was conducted to determine between which groups the

significance was isolated. An alpha level of 0.05 was used and the p values for each comparison are reported in Table 16 and 17 below. If the p value is less than the alpha value, then the sample groups are statistically significantly different, as indicated in column 5 of both tables. Based on whether the t statistic is positive or negative, one can determine which of the two samples had a higher mean. Column 6 indicates which of the two sample groups had superior mechanical properties based on the t statistic results, following establishment of significance.

Table 16: Maximum Force T-Test Values

T-testing: Maximum Force					
Sample 1	Sample 2	P value	Alpha value	Significance	Superior Sample
Hinge	Interlock	0.00194	0.05	Yes	Hinge
Hinge	Control	0.00711	0.05	Yes	Hinge
Interlock	Control	0.09894	0.05	No	N/A

Table 17: Maximum Stress T-Test Values

T-testing: Maximum Stress					
Sample 1	Sample 2	P value	Alpha value	Significance	Superior Sample
Hinge	Interlock	0.00416	0.05	Yes	Hinge
Hinge	Control	0.00804	0.05	Yes	Control
Interlock	Control	0.00094	0.05	Yes	Control

Overall, the Hinge prototype displayed the most favorable parameters based on the areas of significance observed in the data. The maximum force for the Hinge is higher than for both the control and the Interlock. In this regard, the Hinge is favorable because when the forces causing a suture pullthrough are reached, the Hinge device will be able to resist the suture pulling through the device because the device has a higher tolerance for force than the tendon alone. Although the Control displayed the highest value and significance for maximum stress achieved, this does not mean that the Control situation is the most favorable surgical option.

8 CONCLUSION & RECOMMENDATIONS

The final device selection properly addresses the issues for physicians associated with rotator cuff retear surgeries. The limited amount of time that the team had to complete the project lead to some aspects of the design being neglected. Suggestions for future work as well as the conclusion for this project will be discussed in this chapter. These suggestions are to improve mass production/manufacturing strategy, make it work with current surgical techniques, research utility of device for other applications, use of bioadhesives to remove all need of sutures, bioabsorbable material, optimize mechanical properties to be higher, and develop a promotion of biological healing of enthesis surrounding device implementation.

8.1 Conclusions

In conclusion, the final Hinge design for this surgical fastener shows potential to reduce Type I retears in RCR patients with large to massive tears. The final design was chosen and validated using biocompatible and mechanical strength results in order to ensure that the device wasn't subject to mechanical failures when exposed the native forces of the arm, and specifically those associated with the supraspinatus. This claim is supported by the mechanical testing of the Hinge design made of MED610 and the *in vitro* biocompatibility testing results. Tendon samples sutured with this device failed at forces 210% greater when compared to the control. This design can be manipulated to adapt to various tear sizes and potentially expand to other surgical applications. This device is easy to orient into place, it is easily produced by a printable biocompatible material, and all in all, the final device significantly exceeds mechanical strength of the Mason-Allen stitch. As such, it promises to reduce Type I retears *in vivo.*

8.1.1 Achieving Objectives

At the onset of this project, the team defined three major objectives for the device. The objectives are as follows; attachment of tendon to bone should is needed, have similar mechanical properties to the rotator cuff joint, and be biocompatible with the body. The final device shows potential to reduce Type I retears in RCR patients with large to massive tears. It can be easily attached to insertion point and easily oriented into place. MED610 material strength in final device significantly exceeds mechanical strength of Mason-Allen stitch and it promises to reduce Type I retears *in vivo.* In addition to easily being used in the operating room,

the device accounts for biocompatibility in the body and it can be adjusted to fit all patient RCR tears.

As for Tendon-to-Bone adhesion, it was achieved by the usage of suture anchor augmentation which is currently used in order to allow for bone-device interface contact while the tendon healing processes was occurring. The suture anchors were kept in the design as it was the most applicable method to ensure full contact throughout the healing process, as bioadhesives are still under investigation for *in vivo* surgical applications. Sutures will still be used due to the attachment to the anchors, which tie the tendon back to the bone. As previously described, the mechanical properties of the final design were significantly greater than both the alternative design and comparable to the suture-tendon control, thus achieving the second objective. For the final objective the team aimed to accomplish, the material selection for the device. Between MED610 and PLA, both proved to be biocompatible with NIH/3T3 cells. With continued success in *in vitro* studies, further experiments in *in vivo* settings can be conducted to prove complete device safety.

8.1.2 Comparison to Other Devices

Dr. Meislin currently has two patents on both the concept and methods for surgical RCR with a hook-and-loop fastener. This means that there is no current similar product to this fastener on the market, only the current suture-anchors with sutures used for this surgery are used. These documents were initially the guidelines for the preliminary prototypes that were created, as the team was tasked with "attaching the tendon or ligament to a boney structure or to another tendon or ligament portion." As various iterations were developed and adapted, the team veered away from a hook-and-loop fastener concept, thus developing a novel and innovative device. (Meislin, 1999) and (Meislin, 2000).

8.1.3 Limitations

This final design is fully functional, but with any design, there are a few limitations. Throughout all testing, (n=5) runs were used to test samples and devices. Although the data obtained was shown to be statistically significant, further testing would continue to prove the success of the design. The *in vitro* study was not completed in an ISO or ASTM regulated setting and the test conductor was not certified to make the various stitches needed for testing. With all

testing, the group ensured that the standard operating procedures were adhered to; however, these procedures were designed by the engineers creating the device and also may not have been created with accuracy. As with any other *in vivo* device, testing within a patient would be the most beneficial to prove quality and function of the design and get a true representation of its effects in the surrounding area. These data will be obtained through further testing after continued approval of the device. With any device design, limitations exist; however, through sponsor communication and continuous improvement to iterations, these issues can be overcome.

Control points of data collection was a limitation due to the following, sample size, tendon freshness, and preparation of samples. This is a limitation because sample size for sutured-control was an n=5 sample size should be bigger in order to get correct data as well as data analysis. Sample dimensions should be all the same dimensions in regards to length, width, and thickness in order to avoid different sizes of samples and are all the same across the board. Tendon freshness was a limitation as tendons in freezer usually were not fresh were stored in freezer for long period of time could have possibly affected mechanical properties of tendon. A final limitation in control points of data collection were the freeze and thaw cycle this is because tendon samples would be prepared and soaked in saline solution usually a week before tests were ran, this could have possibly affected cell and tendon properties integrity. Future recommendations would be to prepare and test samples all in one day to avoid any outliers in sample preparation.

Although MED610 material selection exceeds mechanical properties compared to that of PLA MED610 is not bioabsorbable. This was a huge limitation because MED610 is not capable of being absorbed into living tissue it also allows for surrounding tissue to remain flexible after the device dissolves.

The final device showed a limitation with current surgical techniques. This limitation is that most commonly used method to treat RCR surgeries is arthroscopic repair it is favored due to small incisions and it is less invasive. The device is too big to fit into an arthroscopic repair surgeon would have to do a mini- open repair surgery. Therefore, the design of the hinge fastener should be altered such that it is compatible with the arthroscopic repair methodology.

In order to address all of these limitations, it is essential to test the final prototype in a patient or cadaver model with the help of an expert surgeon in RCR surgeries. Collecting their

feedback, throughout this process will lead to a final round of iterations that would result in a fully functional device.

8.2 Future Recommendations

8.2.1 Manufacturing

Means of scaling up manufacturing should be sought. Currently, the Objet printer does not print fast enough to satisfy the demands of the market, and as such, a different means, or a different manufacturing device is necessary. The accuracy of each print should also be validated, making sure that each feature is identical between different fasteners.

8.2.2 Current surgical techniques

The design of the fastener should be altered such that it is compatible with the arthroscopic repair methodology. In its current state, it can only feasibly be administered in a mini-open procedure; however, the sutures can be secured with an arthroscope, minimizing the primary incision size slightly. Ideally, the entire procedure should be conducted arthroscopically, and as such the design would need to be compatible with the size limitations of an arthroscope, or the device would need to be flexible enough to be passed through the arthroscope. This would require a change in material.

8.2.3 Utility of Device for Other Applications

Applications other than rotator cuff repair surgery should be identified. RCR surgery, while a demanding application, is a limited market, especially when other types of tissue repair are considered. In the future, the device should be analyzed for its potential usage in Achilles tendon repair, flexor tendon repair in the hand, or even veterinary applications. The FDA approval process is straighter forward for veterinary devices as compared to devices for human use. Under the FDA, this would be considered a Class III device, necessitating a pre-market approval, which is a lengthy document with a long waiting time for approval by the FDA. By pursuing a veterinary market, the device could be brought to the market faster.

8.2.4 Bioadhesives

Currently, the design serves as a suture-anchor augmentation, and only addresses the tendon suture interface. Moreover, the device is to be fastened to the humeral head with suture anchors. In future iterations, the suture-anchors would ideally be eliminated, being replaced with a bioadhesive that would attach the tendon-device construct to the humeral head. Bioadhesives should be tested for both biocompatibility and mechanical strength, ensuring that the adhesives do not elicit cytotoxic responses and the mechanical strengths either meet or exceed that of the suture anchors.

8.2.5 Bioabsorbable Material

MED610 was a biocompatible material available for use in the Objet printer, but is not bioabsorbable. In future designs, a different material should be sought that is both compatible with the 3D printing manufacturing methodology, and is bioabsorbable. This would prevent the need for a follow-up surgery to remove the device once the patient's tendon has completely healed. The material should be mechanically strong for the entire 9 month rehabilitation process, such that the healing tendon does not rupture.

8.2.6 Increase Mechanical Strength Further

In future iterations, the device should be altered such that it is stronger than it is currently. In the case of athletes, a significantly higher force is exerted on the supraspinatus tendon than in other individuals. As such, a higher factor of safety and therefore mechanical strength should be sought in future design iterations.

8.2.7 Promotion of Biological Healing of Enthesis

Currently, the device does not include any features to promote the biological healing of the tendon enthesis, and as such a future design revision could include either biological means or structural means of accomplishing this. Pores could be inserted into the device that allow for cellular migration to the insertion point on the humeral head. In addition, peptides could be used to encourage the tendon to grow onto the device and ultimately onto the humeral head. This could ultimately improve healing time, allowing the patient to return to normal activity sooner than if their surgery was not performed with the fastener.

REFERENCES

Abbi, G., Espinoza, L., Odell, T., Mahar, A., & Pedowitz, R. (2006). Evaluation of 5 knots and 2 suture materials for arthroscopic rotator cuff repair: Very strong sutures can still slip. *Arthroscopy: The Journal of Arthroscopic and Related Surgery, 22*(1), 38-43. doi:10.1016/j.arthro.2005.10.010

Araque-Monrós, M. C., Gamboa-Martínez, T. C., Santos, L. G., Bernabé, S. G., Pradas, M. M., & Estellés, J. M. (2013). New concept for a regenerative and resorbable prosthesis for tendon and ligament: Physicochemical and biological characterization of PLA -braided biomater *Journal of Biomedical Materials Research Part A, 101*(11), 3228-3237. doi:10.1002/jbm.a.34633

Bandholm, T., Rasmussen, L., Aagaard, P., Diederichsen, L., & Jensen, B. R. (2008). Effects of experimental muscle pain on shoulder-abduction force steadiness and muscle activity in healthy subjects. *European Journal of Applied Physiology, 102*(6), 643-650. doi:10.1007/s00421-007-0642-1

Barber, F. A., Herbert, M. A., Beavis, R. C., & Barrera Oro, F. (2008). Suture anchor materials, eyelets, and designs: Update 2008. *Arthroscopy: The Journal of Arthroscopic and Related Surgery, 24*(8), 859-867. doi:10.1016/j.arthro.2008.03.006

Bedi, A., Maak, T., Walsh, C., Rodeo, S. A., Grande, D., Dines, J. S., & Dines, D. M. (2012). Cytokines in rotator cuff degeneration and repair. *Journal of Shoulder and Elbow Surgery, 21*(2), 218-227. doi:10.1016/j.jse.2011.09.020

Bell, C. (2014). Maintaining and troubleshooting your 3D printer.

Bigliani, L. U., Ticker, J. B., Flatow, E. L., Soslowsky, L. J., & Mow, V. C. (1991). The relationship of acromial architecture to rotator cuff disease. *Clinics in Sports Medicine, 10*(4), 823. Retrieved from http://www.ncbi.nlm.nih.gov/pubmed/1934099

Bishop, J., Klepps, S., Lo, I. K., Bird, J., Gladstone, J. N., & Flatow, E. L. (2006). Cuff integrity after arthroscopic versus open rotator cuff repair: A prospective study. *Journal of Shoulder and Elbow Surgery, 15*(3), 290-299. doi:10.1016/j.jse.2005.09.017

Bisson, L. J., & et. al. (2008). Influence of suture material on the biomechanical behavior of suture-tendon specimens: A controlled study in bovine rotator cuff. *Am J Sports Med, 36*(5), 907-912. doi:10.1177/0363546508314793

Black, E. M., Austin, L. S., Narzikul, A., Seidl, A. J., Martens, K., & Lazarus, M. D. (2016). Comparison of implant cost and surgical time in arthroscopic transosseous and transosseous equivalent rotator cuff repair. *Journal of Shoulder and Elbow Surgery / American Shoulder and Elbow Surgeons.[Et al.], 25*(9), 1449-1456. doi:10.1016/j.jse.2016.01.003

Chia, H. N., & Wu, B. M. (2015). Recent advances in 3D printing of biomaterials. *Journal of Biological Engineering, 9*(1), 4. doi:10.1186/s13036-015-0001-4

Colvin, A. C., Egorova, N., Harrison, A. K., Moskowitz, A., & Flatow, E. L. (2012). National trends in rotator cuff repair. *The Journal of Bone & Joint Surgery, 94*(3), 227-233. doi:10.2106/JBJS.J.00739

Cordewener, F. W., van Geffen, M. F., Joziasse, C. A. P., Schmitz, J. P., Bos, R. R. M., Rozema, F. R., & Pennings, A. J. (2000). Cytotoxicity of poly(96 l/4 d-lactide): The influence of degradation and sterilization. *Biomaterials, 21*(23), 2433-2442. doi:10.1016/S0142-9612(00)00111-3

Cummins, C. A., & Murrell, G. A. C. (2003). Mode of failure for rotator cuff repair with suture anchors identified at revision surgery. Journal of Shoulder and Elbow Surgery, 12(2), 128-133. doi:10.1067/mse.2003.21

Favard, L., Bacle, G., & Berhouet, J. (2007). Rotator cuff repair. Joint Bone Spine, 74(6), 551-557. doi:10.1016/j.jbspin.2007.08.003

Gerber, C., Schneeberger, A. G., Beck, M., & Schlegel, U. (1994). Mechanical strength of repairs of the rotator cuff. *The Journal of Bone and Joint Surgery. British Volume, 76*(3), 371.

Ghodadra, N. S., Provencher, M. T., Verma, N. N., Wilk, K. E., & Romeo, A. A. (2009a). Open, mini-open, and all-arthroscopic rotator cuff repair surgery: Indications and implications for rehabilitation. *The Journal of Orthopaedic and Sports Physical Therapy, 39*(2), A6. doi:10.2519/jospt.2009.2918

Gückel, C., & Nidecker, A. (1997). Diagnosis of tears in rotator-cuff-injuries. *European Journal of Radiology, 25*(3), 168-176. doi:10.1016/S0720-048X(97)01171-6

Gundy, S., Manning, G., O'Connell, E., Ellä, V., Harwoko, M. S., Rochev, Y., . . . Barron, V. (2008). Human coronary artery smooth muscle cell response to a novel PLA textile/fibrin gel composite scaffold. *Acta Biomaterialia, 4*(6), 1734-1744. doi:10.1016/j.actbio.2008.05.025

Harryman, D. T., Mack, L. A., Wang, K. Y., Jackins, S. E., Richardson, M. L., & Matsen, F. A. (1991). Repairs of the rotator cuff. correlation of functional results with integrity of the cuff. *The Journal of Bone & Joint Surgery, 73*(7), 982-989.

Hawker, G. A., Mian, S., Kendzerska, T., & French, M. (2011). Measures of adult pain: Visual analog scale for pain (VAS pain), numeric rating scale for pain (NRS pain), McGill pain questionnaire (MPQ), Short -Form McGill p
scale (CPGS), short Form -36 bodily pain sc
and constant osteoarthritis pain (ICOAP). *Arthritis Care & Research, 63*(S11), S252. doi:10.1002/acr.20543

Hurwit, D., Fanton, G., Tella, M., Behn, A., & Hunt, K. J. (2014). Viscoelastic properties of common suture material used for rotator cuff repair and arthroscopic procedures. *Arthroscopy : The Journal of Arthroscopic & Related Surgery : Official Publication of the Arthroscopy Association of North America and the International Arthroscopy Association, 30*(11), 1406-1412. doi:10.1016/j.arthro.2014.05.030

Jeon, E. Y., Hwang, B. H., Yang, Y. J., Kim, B. J., Choi, B. H., Jung, G. Y., & Cha, H. J. (2015). Rapidly light-activated surgical protein glue inspired by mussel adhesion and insect structural crosslinking. *Biomaterials, 67*, 11-19. doi:10.1016/j.biomaterials.2015.07.014

Kim, D. H., ElAttrache, N. S., Tibone, J. E., Bong-Jae, J., DeLaMora, S. N., Kvitne, R. S., & Lee, T. Q. (2006). Biomechanical comparison of a single-row versus double-row suture anchor technique for rotator cuff repair. *The American Journal of Sports Medicine, 34*(3), 407-414. doi:10.1177/0363546505281238

Kim, J., Hong, I., Ryu, K., Bong, S., Lee, Y., & Kim, J. (2014). Retear rate in the late postoperative period after arthroscopic rotator cuff repair. *The American Journal of Sports Medicine, 42*(11), 2606-2613. doi:10.1177/0363546514547177

Kim, K., Shin, H., Cha, S., & Park, J. (2014). Comparisons of retear patterns for 3 arthroscopic rotator cuff repair methods. *The American Journal of Sports Medicine, 42*(3), 558-565.

Lambrechts, M., Nazari, B., Dini, A., O'Brien, M. J., Heard, W. M. R., Savoie, F. H., & You, Z. (2014). Comparison of the cheese-wiring effects among three sutures used in rotator cuff repair. *International Journal of Shoulder Surgery, 8*(3), 81-85. doi:10.4103/0973-6042.140115

Levy, H. J., Uribe, J. W., & Delaney, L. G. (1990). Arthroscopic assisted rotator cuff repair: Preliminary results. *Arthroscopy: The Journal of Arthroscopic & Related Surgery, 6*(1), 55-60. doi://dx.doi.org/10.1016/0749-8063(90)90099-Y

Mahure, S. A., Mollon, B., Shamah, S. D., Zuckerman, J. D., Kwon, Y. W., & Rokito, A. S. (2016). The incidence of subsequent surgery after outpatient arthroscopic rotator cuff repair. *Arthroscopy : The Journal of Arthroscopic & Related Surgery : Official Publication of the Arthroscopy Association of North America and the International Arthroscopy Association, 32*(8), 1531-1541. doi:10.1016/j.arthro.2016.01.039

Mazzocca, A. D., Millett, P. J., Guanche, C. A., Santangelo, S. A., & Arciero, R. A. (2005). *Arthroscopic single-row versus double-row suture anchor rotator cuff repair*

Mendes, G. C. C., Brandão, T. R. S., & Silva, C. L. M. (2007). Ethylene oxide sterilization of medical devices: A review. *AJIC: American Journal of Infection Control, 35*(9), 574-581. doi:10.1016/j.ajic.2006.10.014

Millett, P. J., Mazzocca, A., & Guanche, C. A. (2004). Mattress double anchor footprint repair: A novel, arthroscopic rotator cuff repair technique. *Arthroscopy: The Journal of Arthroscopic and Related Surgery, 20*(8), 875-879. doi:10.1016/j.arthro.2004.07.015

Miyamoto, H., Aoki, M., Hidaka, E., Fujimiya, M., & Uchiyama, E. (2015). Measurement of strain and tensile force of the supraspinatus tendon: Influence of applied torque and joint positioning. *Physiotherapy, 101*, e1015. doi:10.1016/j.physio.2015.03.1882

Najibi, S., Banglmeier, R., Matta, J., & Tannast, M. (2010). Material properties of common suture materials in orthopaedic surgery. *The Iowa Orthopaedic Journal, 30*, 84.

Neer, C. S. (1972). Anterior acromioplasty for the chronic impingement syndrome in the shoulder A PRELIMINARY REPORT. *The Journal of Bone & Joint Surgery, 54*(1), 41-50.

Nicholson, Gregory P. (2002). *Mini open rotator cuff repair* doi:10.1053/otor.2002.36296

Parsons, I., I.M, Apreleva, M., Fu, F. H., & Woo, S. L. -. (2002). The effect of rotator cuff tears on reaction forces at the glenohumeral joint. *Journal of Orthopaedic Research, 20*(3), 439-446. doi:10.1016/S0736-0266(01)00137-1

Randelli, P., Cucchi, D., Ragone, V., de Girolamo, L., Cabitza, P., & Randelli, M. (2015). History of rotator cuff surgery. *Knee Surgery, Sports Traumatology, Arthroscopy*, *23*(2), 344-362. doi:10.1007/s00167-014-3445-z

Reichl, K. K., & Inman, D. J. (2016). Dynamic modulus properties of objet connex 3D printer digital materials. Paper presented at the , *10* 191-198. doi:10.1007/978-3-319-30249-2_15

Rhee, Y., Cho, N., & Parke, C. (2012). Arthroscopic rotator cuff repair using modified mason-allen medial row stitch: Knotless versus knot-tying suture bridge technique. *The American Journal of Sports Medicine, 40*(11), 2440-2447.

Sano, H., Yamashita, T., Wakabayashi, I., & Itoi, E. (2007). Stress distribution in the supraspinatus tendon after tendon repair: Suture anchors versus transosseous suture fixation.*35*, 542+.

Savoie, F. H., Field, L. D., & Nan Jenkins, R. (1995). Costs analysis of successful rotator cuff repair surgery: An outcome study. comparison of gatekeeper system in surgical patients. Arthroscopy: The Journal of Arthroscopic and Related Surgery, 11(6), 672-676. doi:10.1016/0749-8063(95)90107-8

Tempelhof, S., Rupp, S., & Seil, R. (1999). Age-related prevalence of rotator cuff tears in asymptomatic shoulders. *Journal of Shoulder and Elbow Surgery, 8*(4), 296-299. doi:10.1016/S1058-2746(99)90148-9

Vollans, S., & Ali, A. (2016). Rotator cuff tears. *Surgery (Oxford), 34*(3), 129-133. doi:10.1016/j.mpsur.2016.01.005

Yadav, H., Nho, S., Romeo, A., & MacGillivray, J. (2009). Rotator cuff tears: Pathology and repair. *Knee Surgery, Sports Traumatology, Arthroscopy, 17*(4), 409-421. doi:10.1007/s00167-008-0686-8

GLOSSARY

American Society for Testing Materials (ASTM): outlines a variety of testing standards that relate to project completion.

Arthroscopic Surgery: Most common surgical performance conducted by surgeons consisting of three, one-inch incisions for a variety of tools and the arthroscope.

Bioadhesive: Tending to adhere to or cause adhesion in living tissue.

BlueHill Software: Bluehill provides the most powerful and flexible material testing packages available along with an intuitive web-like design. From the simplicity of a basic peak load test to the power required for a complex cyclic test, users will appreciate the minimum learning and training required.

Current Good Manufacturing Practices (cGMP): Standard created by the Food & Drug Administration to ensure ethical responsibility.

Instron 5544: Is a manufacturer of test equipment designed to evaluate the mechanical properties of materials and components, such as universal testing machines.

Interlock Design: One side is equipped with the waves that were used with Hinge Design and the other side had a diamond interlock design to allow for a self-press fitting interface.

Internal Organization of Standardization (ISO): A nongovernmental federation of worldwide bodies that publishes international agreements covering a broad range of services and technologies to promote the use of common standards around the world.

Hinge Design: Prototype evolved from many designs that consists of two folding pieces with three rows of waves and a live hinge to allow for easy line up. The suture holes are reinforced to aid with strength.

MATLAB: Is a fourth-generation programming language and numerical analysis environment. Uses for MATLAB include matrix calculations, developing and running algorithms, creating user interfaces (UI) and data visualization.

MED610: Biocompatible material that is readily available in the (print) lab on the WPI main campus used commonly with dental applications.

Poly(lactic) Acid (PLA): Polymer which is both biodegradable and bioactive, known to be biocompatible with the human body.

Rotator Cuff Repair (RCR): Common orthopedic surgery which aids in the repair of reattaching the torn tendon into the bone.

SolidWorks: A type of 3D computer aided design software that allows for the user to design parts, assemblies, and 2D drawings. SolidWorks allows the user to use tools for sheet metal, weldments, surfacing, and mold tools.

9. APPENDIX

Appendix A: Standard Operating Procedures

A.1 Mechanical Testing: Material Property Testing Protocol for Device Material

1. Purpose
   1.1. This protocol outlines the steps for tensile testing of various 3D printed material samples. Samples are dimensioned and printed in a ‘dog bone’ shape. Testing results will determine which material is favorable for device design.
2. Scope
   2.1. This procedure applies to personnel who conducted the experiment and assess the data collected throughout the design process at Worcester Polytechnic Institute.
3. Responsibility
   3.1. Test Conductor(s):
      3.1.1. Responsible include: gathering all necessary materials needed, preparing Bluehill testing method.
      3.1.2. Conducts test method while recording data necessary for analysis.
   3.2. Data Analyzer(s):
      3.2.1. Assess collected data for various mechanical properties using MATLAB.
      3.2.2. Determine which device is more favorable for the desired application and reference literature for secondary confirmation.
4. Equipment and Materials
   4.1. Equipment
      4.1.1. Instron 5544
      4.1.2. Bluehill software 3.2 equipped computer
      4.1.3. Caliper
      4.1.4. Safety shield
      4.1.5. Safety glasses
      4.1.6. Hex wrench
   4.2. Materials
      4.2.1. 3D printed PLA samples
      4.2.2. 3D printed MED610 samples
5. Definitions
   5.1. Poly(lactic) acid (PLA) is a 3D printable polymer that is known to cause an inflammatory response in vivo.
   5.2. MED610 is biocompatible 3D printable polymer that is commonly used for dental implants. This material is a category C (permanent) biomaterial meaning that it can interface with the human body for greater than 30 days.

5.2.1. SDS can be found at:
http://global72.stratasys.com/~/media/Main/Files/SDS/Dental-and-BIO-Compatible-Materials/SDS_Objet-MED610-Biocompatible-Clear-US.ashx

6. Safety / Caution Statements
   6.1. Safety Equipment: When starting test runs on Instron 5544 always wear safety glasses. Before a test in ran safety shield is placed in front of the Instron.
   6.2. Make sure grips do not touch will lock the Instron and have to reset the whole Instron.
7. Procedures
   7.1. Turn on Instron 5544 machine turn on and off button is located at the right back end of the machine.
   7.2. Log into BlueHill software and open created test method for protocol testing as well as select folder where all data outputs will be saved into.
   7.3. Load dog bone sample onto Instron the sample will be loaded onto the top and bottom grip of the Instron.
   7.4. Once sample is loaded, parameters that are measured with calipers are length, width, and thickness of sample.
   7.5. After parameters are recorded they are inputted into the Bluehill Software.
   7.6. Place shield glass in front of the Instron machine.
   7.7. Balance load and zero extension before test is begun.
   7.8. Press start test. Test will run until failure.
   7.9. When sample reaches failure, Instron should stop test by itself if not manually push stop test in Bluehill Software.
   7.10. Manually hit return sample to put the Instron back to where it begun before test. Save parameters for data collection and analysis.
   7.11. Once all testing is done make sure to log off Bluehill software and turn off Instron machine.
   7.12. Once data is collected in csv files they were loaded onto MATLAB script every MATLAB script changed original length and area.
   7.13. After collecting calculated values max force, max stress, and young’s modulus a statistical analysis ANOVA was ran on all data collection.
   7.14. This procedure was done for both dog bone PLA and MED 610 samples.

A.2 Media Study Testing Protocol for Biocompatibility

1. Purpose
   1.1. The purpose of this document is to provide guidance for conducting elution assays to determine the biocompatibility for a given material.
2. Scope
   2.1. This procedure applies to personnel who; conduct the experiment and assess the data collected throughout the experiment at Worcester Polytechnic Institute.
3. Responsibility
   3.1. Test Conductor(s):
      3.1.1. Responsible for gathering all materials needed to complete a successful trial.
      3.1.2. Running the assays in a clean environment and completing them in a timely manner.
   3.2. Data Analyzer(s):
      3.2.1. Assess collected data for cell counts, cell deaths, and cytotoxicity.
      3.2.2. Determine if the material will harm a living system.
4. Equipment and Materials
   4.1. Media Preparation
      4.1.1. 16 grams of test material
      4.1.2. Mass balance
      4.1.3. 70% Isopropyl Alcohol
      4.1.4. 15 mL and
      4.1.5. 50 mL conical tubes
      4.1.6. 100 mm petri dishes
      4.1.7. Ultraviolet sterilization device
      4.1.8. Autoclaved forceps, stir bars and media bottles
      4.1.9. MediaBattery operated stir plate
      4.1.10. Refrigerator at 4oC
5. Definitions
   5.1. Confluency: Area of cell coverage in a well.
6. Safety / Caution Statements
   6.1. Wear gloves, safety glasses, and lab coats when necessary.
   6.2. Be sure to clean the biohazard safety hood appropriately before and after usage.
   6.3. Always place used cell culture products in the red biohazard bins.
7. Procedures
   7.1. Media Preparation
      7.1.1. Mass out desired amount of material in grams on a weigh boat.
      7.1.2. Place material in a 15 mL conical tube and then fill with 70% Isopropyl alcohol for approximately one to two hours.
      7.1.3. Clean UV sterilizer with 70% IPA before placing device in biohazard hood.

7.1.4. Wipe outside of conical tubes with 70% IPA and place conical tubes in hood. Remove 70% IPA with aspiration pipette and use forceps to put material samples into labeled petri dishes.

7.1.5. Place petri dishes into UV Sterilizer for 30 minutes and close the hood to ensure sterilization process is properly completed. Be sure to turn on the UV light of the hood when completing this step.

7.1.6. In a second hood, start the preparation for complete media.

7.1.7. Complete media should be composed of 10% Fetal Bovine Serum, 1% Penn/Strep, 1% Glutamax and 88% DMEM. Media total based upon desired volume in order to make a concentration of 100mg/mL.

7.1.8. Place stir bar into media bottles along with material samples once the UV sterilization process has been completed.

7.1.9. Take media bottles with sterilized material and stir bars to the stir plate in the 4oC refrigerator. Set the stir plate to 150 rotations per minute.

7.1.10. Leave media and material to soak for one week while periodically checking on it for contamination.

7.1.11. At the end of one week, confirm media has not been compromised and take the material and stir bars out of the bottles.

7.1.12. Use experimental media in section 7.2 to analyze impact of test materials.

7.2. Cell Culture Passaging

7.2.1. The following procedure (7.2.1.1-7.2.1.6) was taken directly from CELL CULTURE PROCEDURES AND PROTOCOLS (Version 11/2010); A MANUAL FOR BIOMEDICAL ENGINEERING MQP MODULE; Prepared by Sakthikumar Ambady, Ph.D Department of Biomedical Engineering Worcester Polytechnic Institute 100 Institute Road Worcester, MA 01609

7.2.1.1. When cells are 70-80% confluent, aspirate medium and wash cells twice with 1X DPBS by adding and then aspirating PBS.

7.2.1.2. Use 1⁄2 the volume of PBS to rinse as there was medium in the dish.

7.2.1.3. Trypsinize cells by adding 1X trypsin EDTA for 3-5 mins. Plates may be returned to the incubator while trypsinizing

7.2.1.4. .Add fresh media to plate, pipette cells up and down to resuspend and break up clumps of cells. Serum in culture medium inactivates trypsin.

7.2.1.5. Add a volume of resuspended cells to fresh medium in a new plate. Alternately, seed a specific number of cells in the total volume prescribed for a particular culture dish.

7.2.1.6. Check growth each day; passage as necessary.

7.3. Cell Staining

7.3.1. Prepare 20mL of DPBS(+) with Hoechst 33342 and Propidium Iodide at concentrations of 0.5ug/mL and 0.2ug/mL, respectively.

7.3.2. Aspirate supernatant from one well, rinse 1x with DPBS(+), and add 3mL of ice cold methanol. Allow the plate to incubate for 10 minutes. This will serve as a positive control.

7.3.3. Aspirate positive control well and any other wells to be stained. Rinse 3x with DPBS(+).

7.3.4. Add 3mL of the DPBS(+) containing the stains to the wells. Cover with foil and incubate for 15 minutes.

7.3.5. Image wells using a Zeiss Fluorescent microscope equipped with the Zen software suite.

7.3.5.1. Phase contrast images should be taken at 40X with an appropriate exposure time.

7.3.5.2. Use the DAPI filter and an appropriate exposure time to image the Hoechst(+) cells.

7.3.5.3. Use the rhodamine filter and an appropriate exposure time to image the Propidium Iodide(+) cells.

7.3.6. Rinse the wells 2x with DPBS(+).

7.3.7. Fix with paraformaldehyde and let stand 10min.

7.3.8. Aspirate wells and add 3mL DPBS(+).

7.4. Experimental Analysis

7.4.1. Compare red fluorescence in the experimental groups against the positive control.

7.4.2. If there is an absence of red fluorescence, there is no apparent cell death.

7.4.3. Remove cells from 3 wells per plate using trypsin-EDTA and pool in one 50mL conical tube.

7.4.4. Take 3 separate 10uL samples from the tube and inject them each into a hemocytometer.

7.4.5. Perform a cell count and compare the cell counts of the experimental groups against the control using a two sample t-test assuming equal variances and an alpha of 0.05.

A.3 Device Testing Protocol for Device Designs

1. Purpose
   1.1. The purpose of this document is to provide guidance on conducting tension testing on device designs in order to determine which is more favorable for the applicable application.
2. Scope
   2.1. This procedure applies to personnel who; conducted the experiment and assess the data collected throughout the design process at Worcester Polytechnic Institute.
3. Responsibility
   3.1. Test Conductor(s):
      3.1.1. Responsible for gathering all materials needed to a successful trial as well as setting up the test method in BlueHill Software before conducting tests.
      3.1.2. Conducts test method while recording data necessary for analysis.
   3.2. Data Analyzer(s):
      3.2.1. Assess collected data for various mechanical properties using MatLAB
      3.2.2. Determine which device is more favorable for the desired application and reference literature for secondary confirmation.
4. Equipment and Materials
   4.1. Instron 5544 with BlueHill Software 3.61
   4.2. N =5 per each device being tested
   4.3. Bovine tendons
   4.4. Blue surgical drape material
   4.5. FiberWire Number 2 Sutures: REF AR-7202 Lot 15630
   4.6. Preparation Tools
      4.6.1. Caliper
      4.6.2. Scalpel
      4.6.3. Scissors
      4.6.4. Saline
      4.6.5. Glass beaker
      4.6.6. Mock bone-tendon interface
5. Definitions
   5.1. Mason-Allen Stitch: Currently used in rotator cuff repair surgeries that allows the surgeon to reinforce the attachment site for strength.
6. Safety / Caution Statements
   6.1. Wear gloves, lab coat and goggles when conducting experiment.
   6.2. Be sure to handle the scalpel properly.
   6.3. Line Instron and surrounding area with blue surgical drape material.
   6.4. Always put up safety glass before running the experiment.
   6.5. Spray down machine with Amphyl when testing is completed.
7. Procedures

7.1. Preparation of Tendon

7.1.1. Place the frozen specimen into the glass beaker and submerge it in saline for approximately one hour. Once thawed, the sheath can be trimmed off to reveal the tendon itself by cutting each end to start the removal process.

7.1.2. After the tendon sheath has been removed, the connective tissue can be cut away from the tendon, leaving behind a clean specimen.

7.1.3. The tendon is now able to be cut down to have a cross sectional area of 6 millimeters by 2.5 millimeters in order to prevent slippage between the grips.

7.1.4. If the tendons are not being used immediately used they can be soaked in saline solution and wrapped in gauze, folded in tin foil and labeled in a biohazard storage bag.

7.2. Experimentation of Control

7.2.1. Tendon Mechanical Properties

7.2.1.1. Line the Instron with Blue Chuck paper.

7.2.1.2. The control of this experiment will be a N = 5 test of only the tendon in the Instron grips with the precreated BlueHill Software testing file.

7.2.1.3. Wrap the ends of the tendon with a piece of gauze and load the sample in the top grip.

7.2.1.4. Lower the fixture to line up the sample with bottom grip and then make sure that side of the tendon is tightened into place.

7.2.1.5. Extend the Instron grips to ensure that the tendon is fully elongated and relaxed.

7.2.1.5.1. Apply a tear load of 5 Newtons and Zero the displacement.

7.2.1.6. Safety Checks:

7.2.1.6.1. Check the safety stops and mount the safety shield.

7.2.1.7. Run the test. Record and save all results and data.

7.2.2. Tendon Pull Through Strength with FiberWire Sutures

7.2.2.1. Line the Instron with blue biohazard paper.

7.2.2.2. The control of this experiment will be a N = 5 test of only the tendon connected to sutures in the Instron grips with the precreated BlueHill Software testing file.

7.2.2.3. To suture the tendon, a Mason-Allen stitch will be used to determine the pull out failure strength of the suture-tendon interface. This stitch should be made approximately 5 millimeters from the bottom of the tendon.

7.2.2.4. After the 3 of pass-trough’s has been completed, a loop will be knotted off from the suture in order to hook it onto the screw that will be locked into the base grip of the Instron.

7.2.2.5. Wrap the unsutured end of the tendon with a piece of gauze and load the sample in the top grip.

7.2.2.6. Lower the fixture to line up the looped sample with bottom grip on the screw.

7.2.2.7. Extend the Instron grips to ensure that the tendon is fully elongated and relaxed.

7.2.2.7.1. Apply a tear load of 5 Newtons and Zero the displacement.

7.2.2.8. Safety Checks:

7.2.2.8.1. Check the safety stops and mount the safety shield.

7.2.2.9. Run test and save data.

7.3. Experimentation of Devices

7.3.1. Hinge Prototype

7.3.1.1. Prepare N=5 bovine tendons for testing as described in steps 7.1 through 7.2.

7.3.1.2. Put device flat on a cutting board with tendon on one half of the device with 3 noncontact waves at the bottom as seen below. Have suture ready for preparation with a hemostat.

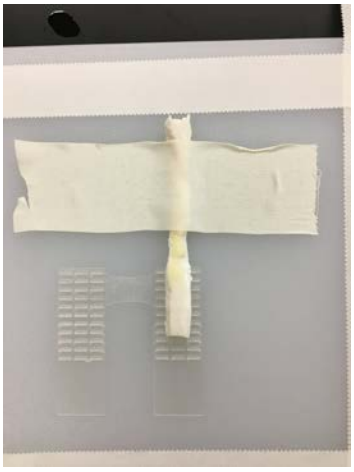

Figure 1. Device Tendon Alignment

7.3.1.3. Conduct 2 crossing stitches per group of 4 holes between the device and tendon. Repeat for a second group of 4 holes.

2a. 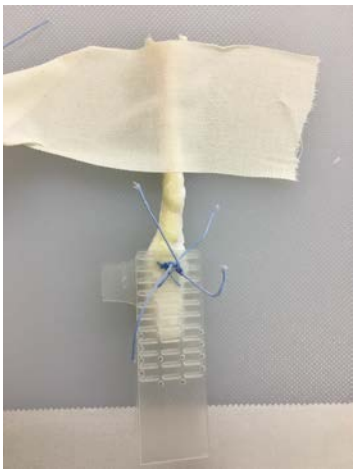 2b. 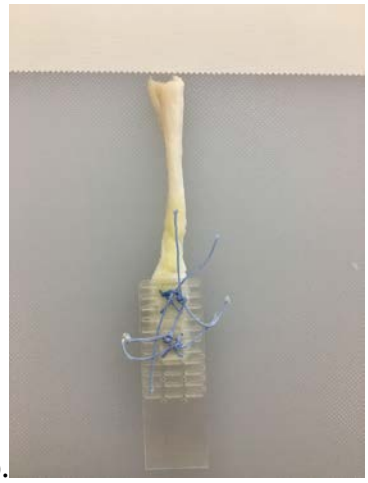

Figure 2a. Device Tendon (1) Group Cross 2b. Device Tendon (2) Group Cross

7.3.1.4. Once device and tendon is locked into place, Instron testing can be conducted following step 7.2.2.5 through 7.2.2.9

7.3.2. Press Fit Prototype

7.3.2.1. Prepare N=5 bovine tendons for testing as described in steps 7.1 through 7.2.

7.3.2.2. Put tendon flat on a cutting board with flat side of device facing up. Three lengths of wholes are lined up on the tendon and at the end of the tendon, there is one row of waves. Have suture ready for preparation with a hemostat for first suture pass-through.

3a. 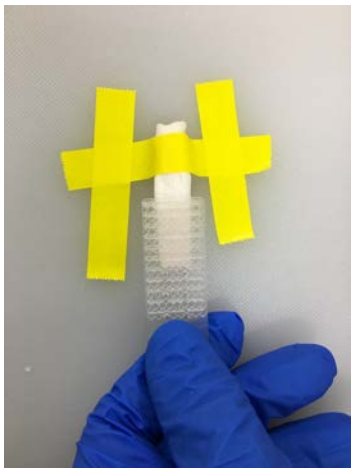 3b. 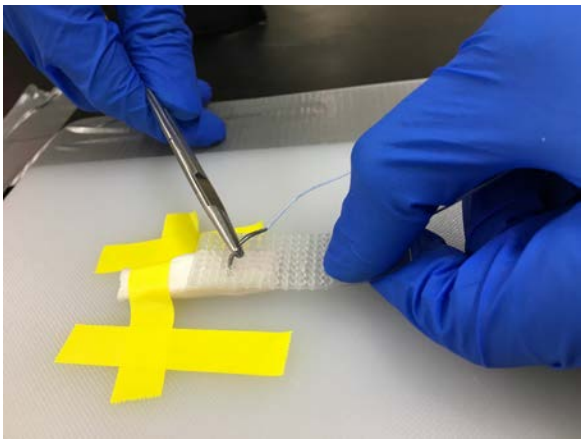

Figure 3a. Device Tendon Alignment 3b. Needle Entry into Hole

7.3.2.3. Conduct 2 crossing stitches per group of 4 holes between the device and tendon.

4a.  4b. 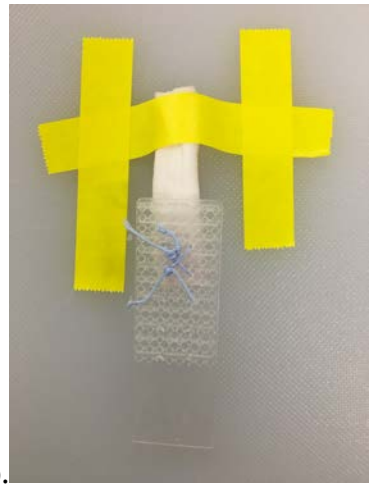

Figure 4a. Device Tendon (1) Group Cross 4b. Device Tendon (2) Group Cross

7.3.2.4. Complete 1 horizontal stitch above the cross hatching stitch.

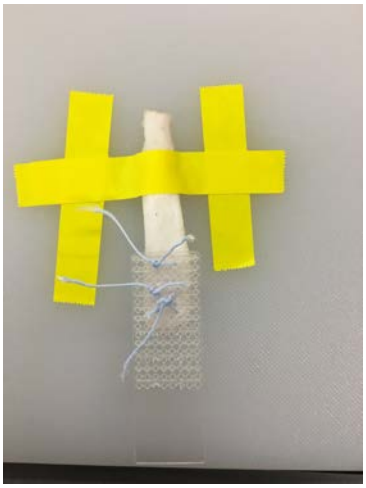

Figure 5. Completed View of Stitches

7.3.2.5. Score the end of the testing device to allow for ease of break off. This is done in order to allow the Instron to only grip one end of the device, verse the two ends of the device.

6a. 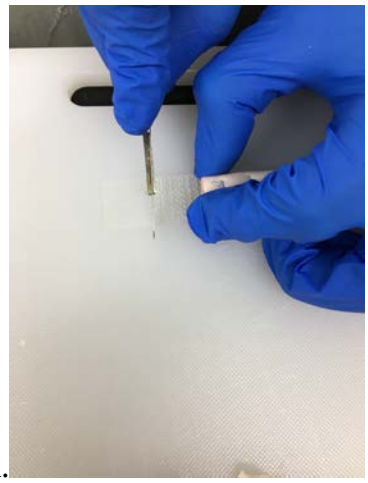 6b. 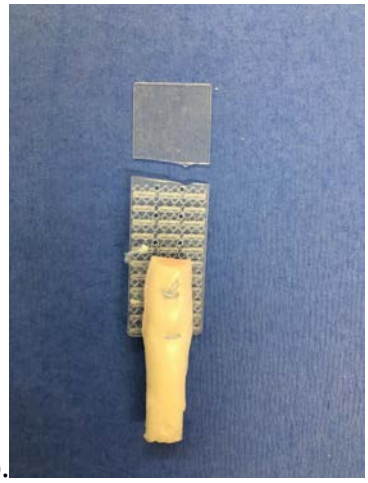

Figure 6a. Pre-Scoring 6b. Post-Scoring

7.3.2.6. Attach partnering side of the device on the diamond press interface.

7.3.2.7. Once device and tendon is locked into place, Instron testing can be conducted following step 7.2.2.5 through 7.2.2.9

Appendix B: Transcript of Client Feedback Meeting

Evaluation of Final 3 Designs (21Mar17)

Interlock: Likes overall proof of concept of interface “clicking into place”, suggests to evaluation pullout force and if the length of the device is changed, would the results be similar? Experiment with a bioadhesive and it will become more marketable.

Clamp: Understands overall design and concept however would not sell well due to size and failure of teeth to hold the tendon into place.

Hinge: Enjoys idea of teeth holding tendon together, but doesn’t like the idea of it’s implantation, seems to expect more of a Velcro-like concept like the interlock.

Overall: Sees potential for flexibility of material to work cohesively with RCR and is impressed with the resolution of the prototypes. Understands that while he likes the Interlock design better, the Hinge has stronger mechanical properties which will aid in preventing Type I retears.

Appendix C: Material Properties & *In Vitro* Simulation Data Table

Test Type	Material	Sample	Width (mm)	Thickness (mm)	Grip to Grip (mm)	Rod to Grip (mm)	Suture Diameter (mm)	Suture Passage	Area (mm^2)	Average Area (mm^2)	Area S.D.	Strain Rate (mm/min)	Max Force (N)	Average Max Force (N)	Max Force S.D.	Max Stress (MPa)	Average Max Stress (MPa)	Max Stress S.D.	Young's Modulus (MPa)	Average Youngs' Modulus (MPa)	Young's Modulus S.D.
Controls	Bovine Tendon	BovineSuture_Sample_1	10.2700	3.9700	112.5900	98.9000	0.5000	3.0000	5.9500			50.0000	91.1120			15.3130			28.9110		
		BovineSuture_Sample_2	8.4000	5.5800	81.5000	67.3700	0.5000	3.0000	8.3700			50.0000	259.5080			31.0400			114.1750		
	Suture Mason Allen	BovineSuture_Sample_3	8.0800	4.1500	72.5900	58.5200	0.5000	3.0000	6.2200	6.8900	1.0738	50.0000	164.1350	177.7570	60.6647	26.3670	25.3592	6.0084	128.9660	92.9666	56.7900
		BovineSuture_Sample_4	8.0800	4.1500	84.3200	71.1300	0.5000	3.0000	6.2200			50.0000	177.7070			28.5470			155.6700		
		BovineSuture_Sample_5	9.7800	5.1300	106.4200	93.2000	0.5000	3.0000	7.6900			50.0000	196.3230			25.5290			37.1110		
Experimental	Hinge Wave Design 1	HingeWave_Sample_1	9.0400	6.5100	41.5800	N/A	0.4000	8.0000	28.6000			50.0000	418.9300			14.6400			53.8500		
		HingeWave_Sample_2	6.9600	7.1500	41.5100	N/A	0.3800	8.0000	28.1200			50.0000	349.5500			12.4300			15.1900		
		HingeWave_Sample_3	14.0900	7.0300	40.2600	N/A	0.3900	8.0000	29.5600	28.4000	1.4724	50.0000	398.3300	361.7280	48.0106	13.4700	12.7120	1.3492	71.6800	54.0720	22.6669
		HingeWave_Sample_4	10.4600	7.3900	40.2600	N/A	0.5300	8.0000	29.6800			50.0000	344.6700			11.6100			65.8700		
		HingeWave_Sample_5	8.8900	7.4200	39.9500	N/A	0.4000	8.0000	26.0400			50.0000	297.1600			11.4100			63.7700		
	Interlock Design 2	BarbPress_Sample_1	11.5600	8.8200	68.0900	N/A	0.4100	6.0000	26.4600			50.0000	105.9530			4.0000			37.3140		
		BarbPress_Sample_2	11.0000	8.7200	67.5500	N/A	0.4100	6.0000	26.1600			50.0000	134.3400			5.1300			26.6450		
		BarbPress_Sample_3	9.6600	7.1600	89.1700	N/A	0.4100	6.0000	21.4800	23.5620	2.5166	50.0000	135.0700	135.7364	44.0734	6.2800	5.8600	2.2472	45.9190	35.9144	21.9554
		BarbPress_Sample_4	9.4000	7.3200	60.4800	N/A	0.4500	6.0000	21.9600			50.0000	95.2090			4.3300			5.3690		
		BarbPress_Sample_5	10.7400	7.2500	59.9400	N/A	0.4100	6.0000	21.7500			50.0000	208.1100			9.5600			64.3250		

Appendix D: Secondary References

American Society for, Testing Materials. (2016). *Annual book of ASTM standards 2016: Medical devices and services. medical and surgical materials and devices (I): E667-F2477. section 13. vol. 13.01* ASTM International.

Faludi, J. (2013). Environmental impacts of 3D printing. Retrieved from https://sustainabilityworkshop.autodesk.com/blog/environmental-impacts-3d-printing

FDA (2014). (4th ed.) Oxford University Press.

International Symposium on Engine Coolant Technology, ASTM Standards and Engineering Digital Library, & ASTM International. (2004). Journal of ASTM international. *Journal of ASTM International.*

ISO. (2006). *Iso11737-1*

ISO. (2016). *Use of international standard ISO 10993-1, 'biological evaluation of medical devices--part 1: Evaluation and testing within a risk management process"; guidance for industry and food and drug administration staff; availability.* (No. 81). Lanham: Federal Information & News Dispatch, Inc.

Lutz Tool Company . "Gorilla Glue | Gorilla Glue." *Original Polyurethane Formula | Waterproof Glue*. N.p., 1999. Web. 10 Oct. 2016.

Medical technology spotlight: Select USA. (2017).

Meislin, R. J. (1999). *Surgical repair with hook-and-loop fastener* Retrieved from http://worldwide.espacenet.com/searchResults?DB=EPODOC&compact=false&query=US5906617

Meislin, R. J. (2000). *Method for surgical repair with hook-and-loop fastener* Retrieved from http://worldwide.espacenet.com/searchResults?DB=EPODOC&compact=false&query=US6039741

Products in the news: High-heat and -impact PLA for 3D printing yields tight tolerances and less shrinkage and. (2015).

Six Sigma. (2017). About us, six sigma training.

Thul, 1979. "3M™ Vetbond™ Tissue Adhesive."3M, 1979. Web. 10 Oct. 2016